ADA 025136

# The AURORA Dosimetry System

## March 1976

RESEARCH
DEVELOPMENT
ENGINEERING

U.S. Army Materiel Command
**HARRY DIAMOND LABORATORIES**
Adelphi, Maryland 20783

```
-- 1 -   AD NUMBER: A025136
--48 -   SBI SITE HOLDING SYMBOL:       RSIH
-- 2 -   FIELDS AND GROUPS: 9/1, 18/4
-- 3 -   ENTRY CLASSIFICATION:    UNCLASSIFIED
-- 5 -   CORPORATE AUTHOR: HARRY DIAMOND LABS   ADELPHI MD
-- 6 -   UNCLASSIFIED TITLE:      THE AURORA DOSIMETRY SYSTEM.
-- 8 -   TITLE CLASSIFICATION:    UNCLASSIFIED
-- 9 -   DESCRIPTIVE NOTE: TECHNICAL REPT.,
--10 -   PERSONAL AUTHORS: KERRIS,KLAUS G. ;
--11 -   REPORT DATE:        MAR   , 1976
--12 -   PAGINATION:      48P    MEDIA COST:  $  6.00 PRICE CODE:    AA
--14 -   REPORT NUMBER:     HDL-TR-1754
--16 -   PROJECT NUMBER:    DNA-NWET-L37IAXY
--17 -   TASK NUMBER:       X970
--20 -   REPORT CLASSIFICATION:  UNCLASSIFIED
--23 -   DESCRIPTORS:       *RADIATION MEASURING INSTRUMENTS, *GAMMA RAYS,
--         *ELECTRONIC EQUIPMENT, MILITARY EQUIPMENT, NUCLEAR WEAPONS, NUCLEAR
--         EXPLOSION DAMAGE, RADIATION EFFECTS, DOSIMETRY
--24 -   DESCRIPTOR CLASSIFICATION:    UNCLASSIFIED
--25 -   IDENTIFIERS:       *AURORA SYSTEM, *THERMOLUMINESCENT DOSIMETERS
--26 -   IDENTIFIER CLASSIFICATION:    UNCLASSIFIED
--          <<P FOR NEXT PAGE>> OR <<ENTER NEXT COMMAND>>
                                       *MSG RECEIVED*
1a ROW=24 COL= 01          <Ctrl>H For Help                    N   Poll
```

| REPORT DOCUMENTATION PAGE | | READ INSTRUCTIONS BEFORE COMPLETING FORM |
|---|---|---|
| 1. REPORT NUMBER<br><br>HDL-TR-1754 | 2. GOVT ACCESSION NO. | 3. RECIPIENT'S CATALOG NUMBER |
| 4. TITLE *(and Subtitle)*<br><br>The AURORA Dosimetry System | | 5. TYPE OF REPORT & PERIOD COVERED<br><br>Technical Report |
| | | 6. PERFORMING ORG. REPORT NUMBER |
| 7. AUTHOR*(s)*<br><br>Klaus G. Kerris | | 8. CONTRACT OR GRANT NUMBER*(s)* |
| 9. PERFORMING ORGANIZATION NAME AND ADDRESS<br><br>Harry Diamond Laboratories<br>2800 Powder Mill Road<br>Adelphi, MD 20783 | | 10. PROGRAM ELEMENT, PROJECT, TASK AREA & WORK UNIT NUMBERS<br>Program: 62710H<br>Subtask: L37IAYX970<br>Work Unit: 04 |
| 11. CONTROLLING OFFICE NAME AND ADDRESS<br><br>Director<br>Defense Nuclear Agency<br>Washington, DC 20305 | | 12. REPORT DATE<br><br>March 1976 |
| | | 13. NUMBER OF PAGES<br>48 |
| 14. MONITORING AGENCY NAME & ADDRESS*(if different from Controlling Office)* | | 15. SECURITY CLASS. *(of this report)*<br><br>UNCLASSIFIED |
| | | 15a. DECLASSIFICATION/DOWNGRADING SCHEDULE |

16. DISTRIBUTION STATEMENT *(of this Report)*

Approved for public release; distribution unlimited.

17. DISTRIBUTION STATEMENT *(of the abstract entered in Block 20, if different from Report)*

19. KEY WORDS *(Continue on reverse side if necessary and identify by block number)*

Dosimetry
Dosimeter
Radiation dosimetry
Thermoluminescent dosimeter
Equilibrium dose

20. ABSTRACT *(Continue on reverse side if necessary and identify by block number)*

Making dose and dose-rate measurements at AURORA, a high-intensity bremsstrahlung facility, posed some unusual problems because of the large number of measurements normally required for each pulse and the large dose range encountered there. These problems were solved by careful choice of thermoluminescent dosimeters and extensive automation in the readout and data reduction processes.

DD FORM 1 JAN 73 **1473** EDITION OF 1 NOV 65 IS OBSOLETE

The AURORA simulator is designed to provide short pulses of high energy bremsstrahlung over volumes large enough to irradiate entire weapon systems or large subsystems uniformly. Typically, 120-ns pulses of 20 to 50 krads(Si) can be delivered into a 1-m cube. Because of the large irradiation volume, it is not unusual for an experimenter to desire dose measurements at up to 200 locations within his system, sometimes with a pulse repetition rate of four pulses per day. Most frequently, the dose data are requested in rads(Si).

A dosimetry system for this facility therefore required the following characteristics:

(a) Ability to measure equilibrium and nonequilibrium silicon dose

(b) Useful dynamic range extending from 1 to $10^5$ rads(Si)

(c) Independence of dose rate up to $5 \cdot 10^{11}$ rads(Si)/s

(d) Capability of reading, processing, and recording up to 800 data points per day.

This report describes a dosimetry system designed to fit these requirements. The rationale for our choice of thermoluminescent dosimeters, characteristics of these dosimeters, design of instrumentation and data analysis, precision and accuracy are described.

CONTENTS

3

## FIGURES

## TABLE

## 1.  INTRODUCTION

AURORA, a generator of intense bremsstrahlung pulses, is used principally for simulating the effects of a nuclear weapon prompt gamma pulse on military electronic systems. AURORA's unique feature is its extremely high volumetric dose output; it can deliver 25 krads(Si) throughout a 1 m-diam, 1 m-long cylindrical volume, or 50 krads(Si) throughout a 25-cm sphere. AURORA is located at Adelphi, MD, and is operated by the Harry Diamond Laboratories for the Defense Nuclear Agency.

This report describes the techniques and instruments used at AURORA for measuring the radiation dose and dose rate. This is, of course, important to experimenters at AURORA for understanding and interpreting their dose data. But, more than this, it is hoped that this information will be useful also to anyone who must do dosimetry at the many other pulsed bremsstrahlung facilities that now exist or are planned.

The present report describes in detail the experimental techniques of dosimetry as they are now implemented at AURORA. It thus complements, but does not significantly reiterate, the contents of two other reports concerned with AURORA dosimetry. The first[1] describes the experiments and rationale that led to the eventual adoption of the AURORA dosimetry system as it now exists. It provides especially valuable insight into the characteristics of the various thermoluminescent phosphors and their applicability to the AURORA dosimetry problem. Some of this information can be found also elsewhere.[2] Another report (unpublished) does not dwell on technique per se, but describes the radiation output characteristics of AURORA to the extent that they are known at this time. These three reports together tell the whole AURORA dosimetry story.

Readers who are interested in the general characteristics of the AURORA simulator and facility operations and instrumentation should consult the AURORA Facility brochure (available from author).

## 2.  DOSIMETRY THEORY

This chapter is not intended to be a definitive treatise of dosimetry theory. The aim is to present just enough theoretical background here to justify some of the concepts and equations used in the following chapters. Readers desiring a more rigorous treatment of

[1]*F. H. Attix, Dosimetry for the Aurora Facility, Final Report, Naval Research Laboratory, Washington, DC, NRL Memorandum Report 2552, Revised (March 1973).*

[2]*S. G. Gorbics, F. H. Attix, and K. Kerris, Thermoluminescent Dosimeters for High-Dose Applications, Health Physics, 25 (1973), 499.*

dosimetry theory are urged to consult other sources for general background and a discussion of charge particle equilibrium[3,4] and for Bragg-Gray cavity theory. [3,5]

Radiation dosimetry is the measurement of the energy deposited in matter by radiation. The energy per unit mass deposited in an infinitesimal volume of a material is called the dose. That is, if we let $\Delta E_D$ be the energy deposited in a very small volume of a substance of mass $\Delta m$, the dose is given by

$$D = \frac{\Delta E_D}{\Delta m} .$$ (1)

The unit of dose is the rad, which is equal to 100 ergs/gram by definition. Since the quantity of energy absorbed from any given radiation field depends on the nature of the material, it is necessary to specify which particular material one is referring to when talking about dose. This reference is always made by a parenthetical notation immediately following the name of the units; e.g., rad(air). Thus, if exposure to a certain source of radiation results in 600 ergs being absorbed by 1 gram of silicon, we say that the dose was 6 rads(Si).

In the particular situation of interest at AURORA, that is, where the radiation consists of energetic photons, energy is deposited in matter in a two-step process. First, a photon transfers energy to an electron in the material by the photoelectric, Compton, or pair-production process. Then this electron transfers its kinetic energy to the material via ionization processes.

The dose deposited in an infinitesimal volume of material in this situation is given by equation (1) where

$$\Delta E_D = \Delta E_E - \Delta E_L$$ (2)

[3]F. H. Attix, W. C. Roesch, and E. Tochilin, Radiation Dosimetry, 2nd Ed., Academic Press, New York (1966).

[4]F. H. Attix, Basic Gamma-Ray Dosimetry, Health Physics, 15 (1968), 49.

[5]Robley D. Evans, The Atomic Nucleus, McGraw-Hill Book Co., New York (1955), 723.

in which $\Delta E_E$ is the energy entering the mass $\Delta m$; $\Delta E_L$ is the energy leaving it. This situation is pictured in figure 1(a). Imagine a given (not necessarily microscopic) volume of material exposed to high-energy photon radiation and the need to know the dose at a point P. If $\Delta m$ is the infinitesimal mass of material surrounding P, then the dose is given by equations (1) and (2) where equation (2) becomes

$$\Delta E_D = \Delta E_E(e) - \Delta E_L(e) + \Delta E_E(\gamma) - \Delta E_L(\gamma) . \qquad (3)$$
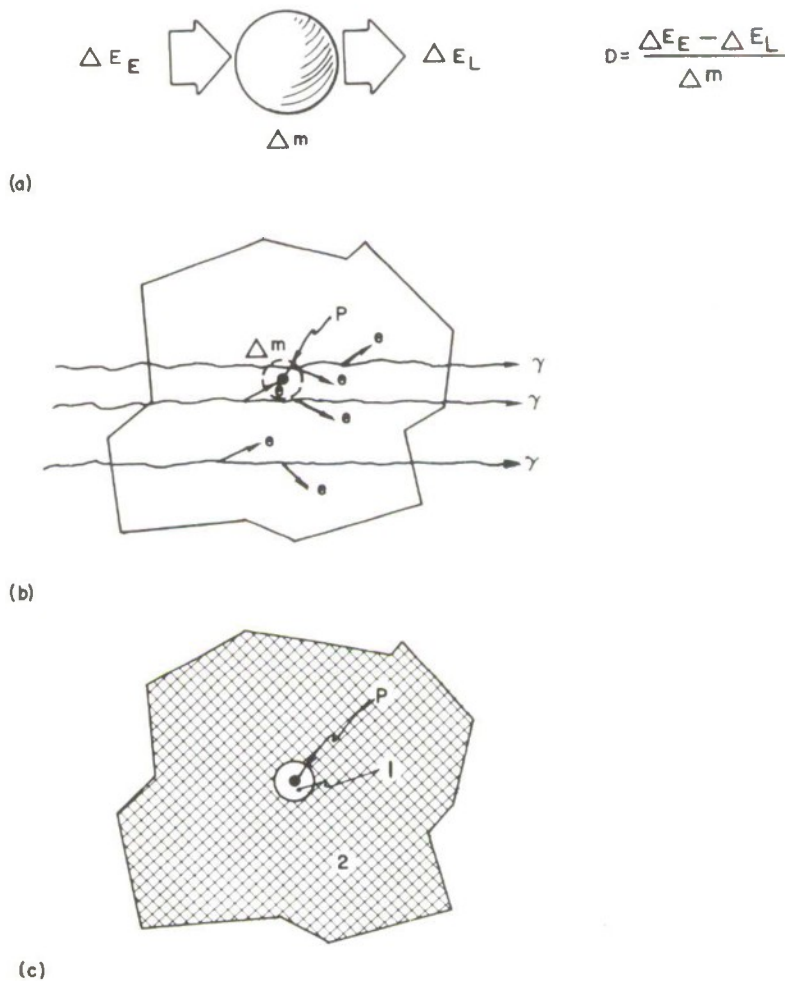


(a)



(b)



(c)

Figure 1. Dose: (a) definition and applications to (b) charged particle equilibrium and (c) Bragg-Gray cavity theory.

The parenthetical modifiers refer to electrons (e) and photons ($\gamma$). This process is illustrated in figure 1(b). All these $\Delta E$'s are difficult to identify and calculate in practice. However, equation (3) can be significantly simplified for a condition that is of considerable practical importance to dosimetry, namely, that of charged particle equilibrium (CPE).

## 2.1 Charged Particle Equilibrium

Considering figure 1(b), when point P is very near the left side of the indicated volume, $\Delta E_E(e)$ will be very small, because there is little material in front of $\Delta m$ from which electrons can be scattered into $\Delta m$. Considering points farther to the right, a point in the material is reached where as many electrons are scattered into $\Delta m$ as are scattered out. This is the condition for charged particle equilibrium:

$$\Delta E_E(e) = \Delta E_L(e) \ .$$ (4)

When this condition is satisfied, equation (3) reduces to

$$\Delta E_D = \Delta E_E(\gamma) - \Delta E_L(\gamma)$$ (5)

for CPE. But, generally,

$$\Delta E_L(\gamma) = \Delta E_E(\gamma) \exp\left(-\left(\mu_{en}/\rho\right)\rho\Delta t\right)$$ (6)

where $\Delta t$ is the thickness of material traversed, and $\mu_{en}/\rho$ is the mass energy absorption coefficient. For small $\mu_{en}/\rho$, equation (6) becomes

$$\Delta E_L(\gamma) \simeq \Delta E_E(\gamma)\left(1-\left(\mu_{en}/\rho\right)\rho\Delta t\right) \ .$$ (7)

If this result is put into equation (5),

$$\Delta E_D = \Delta E_E(\gamma)\left(\mu_{en}/\rho\right)\rho\Delta t$$ (8)

for CPE, and from equation (1)

$$D = \frac{\Delta E_D}{\Delta m} = \phi_\gamma \left( \mu_{en}/\rho \right) *$$
(9)

for CPE, where

$$\phi_\gamma = \frac{\Delta E_E(\gamma)}{\Delta A} ,$$

the incident photon energy fluence, and $\Delta A$ is an element of area.

As an important consequence of equation (9), the ratio of the equilibrium dose in material 1 to the equilibrium dose in material 2, for the same incident monoenergetic photon fluence, is given by

$$\frac{D_1}{D_2} = \frac{\left( \mu_{en}/\rho \right)_1}{\left( \mu_{en}/\rho \right)_2}$$
(10)

for CPE.

## 2.2  Bragg-Gray Cavity Theory

Assume now that the infinitesimal volume in figure 1(b) is not of the same substance as the surrounding material, but is a small cavity filled with some other material. Let the cavity material be 1; call the surrounding material 2. This is illustrated in figure 1(c). Further, assume that electronic equilibrium (CPE) exists, and that the dimensions of the cavity are small with respect to the range of the secondary electrons.

---

*This is only true for monoenergetic photons. When there is a photon energy spectrum, $\phi_\gamma$ (E), the correct expression is*

$$D = \int_0^{E_{max}} \frac{d\phi_\gamma(E)}{dE} \left( \mu_{en}(E)/\rho \right) dE,$$

*where*

$$\frac{d\phi_\gamma(E)}{dE}$$

*is the differential photon energy fluence spectrum.*

Subject to these restrictions, the ratio of the dose absorbed by the cavity material to that absorbed by the surrounding material is

$$\frac{D_1}{D_2} = \frac{S_1}{S_2} \tag{11}$$

where $S_1$ is the effective mass stopping power,

$$\frac{1}{\rho} \frac{dE}{dx} \ (\text{MeV-cm}^2/\text{gram}) \ ,$$

for the electron spectrum generated by the photon field in material 1. This equation will be applied to finding the dose absorbed by a small thermoluminescent dosimeter (TLD) in a thick-walled capsule.

## 3. TYPES OF DOSIMETERS

The problem of what dosimeter to choose for use at AURORA was circumscribed by the probable requirements of experimenters doing large systems tests. These requirements were

(a) Small size, to fit into electronic modules with a high component packing density

(b) Capability of making a large number of measurements per shot, possibly 200

(c) Measurements of dose in rads(Si) or rads(Ta)

(d) Useful dose range from 1 to $10^5$ rads(Si).

Clearly, the dosimeters had to be passive, since instrumenting 200 active channels with cables and recording equipment would have been prohibitive. The size requirement ruled out chemical dosimeters and ionization chambers (not seriously considered, anyway). Finally, the extremely large dose range eliminated glass rods, radiachromic dye films, and photographic film, leaving the TLD's as the only reasonable choice. They are a good choice for other reasons as well. They are available from several manufacturers in a large variety of compositions and physical form. The TLD readout instruments are also available from a number of manufacturers as standard catalog items. The TLD's are inexpensive and easy to use and retain dose information for years at room temperature. Further, the quality control in their manufacture is

now such that dose measurements can be made with a precision of ±2 to 4 percent (at 1 σ) without use of any unusual techniques (such as mass screening or individual precalibration).

Thermoluminescent (TL) phosphors are normally salts of alkali or alkaline-earth metals, quite often doped with trace quantities of other elements. Some of the more commonly used phosphors are lithium fluoride, LiF; manganese-doped lithium tetraborate, $Li_2B_4O_7$:Mn; manganese-doped calcium fluoride, $CaF_2$:Mn; dysprosium-doped calcium fluoride, $CaF_2$:Dy; and manganese-doped calcium sulfate, $CaSO_4$:Mn. The mechanism by which these materials store energy proportional to dose and release it later for readout is similar for all of them.

Thermoluminescent phosphors are insulators with electron trapping centers in the band gap. Ionizing radiation imparts enough energy to valence electrons to raise them to the conduction band, whence many are trapped. In a good TL phosphor, these trapped electrons are stable at room temperature and remain trapped for a long time. The density of such trapped electrons is proportional to the energy deposited in the material per unit mass, that is, the dose. To read the dosimeter, the material is heated to a sufficiently high temperature to thermally excite the trapped electrons into the conduction band, whence they return to the valence band with the emission of light. This process is diagrammed in figure 2.

The light output as a function of phosphor temperature is shown for a representative phosphor in figure 2(b). Several peaks are seen corresponding to various trap depths. Either the peak intensity or the integral under the curve can be used as a measure of the radiation dose. When the integral is used, low temperature peaks corresponding to shallow traps can introduce variations into the data by becoming partly de-excited at room temperatures. When this is the case (as it is for LiF), better reproducibility can be achieved either by removing the peaks by a low temperature preannealing step or by electronically integrating only between two preset temperatures, $T_1$ and $T_2$, as indicated by the shading in figure 2(b).

Of all the phosphors mentioned above, $CaF_2$:Mn was chosen for routine dosimetry at AURORA for the following reasons. Figure 3 shows the thermoluminescence (TL) as a function of exposure for the three phosphors LiF, $CaF_2$:Mn, and $Li_2B_4O_7$:Mn. The $CaF_2$:Mn and $Li_2B_4O_7$:Mn are usable at much higher exposures than LiF, about $10^6$ versus about $2 \times 10^5$ R for LiF. Also, the TL response of LiF departs farthest from linearity, whereas $CaF_2$:Mn is the most linear. It has also been

11
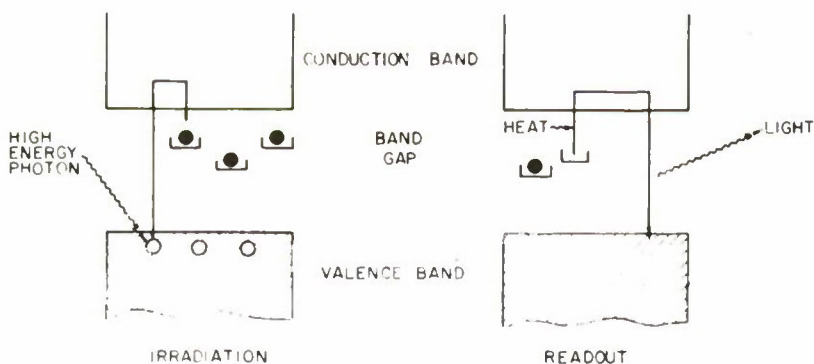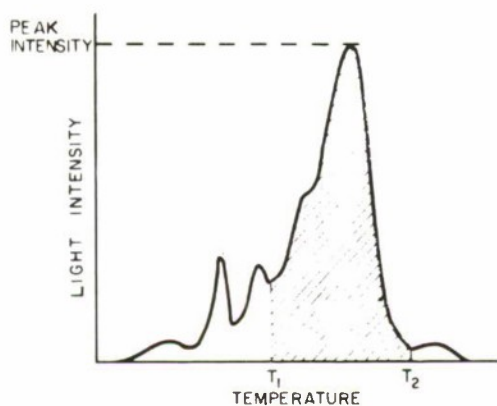
Figure 2. The radio-thermoluminescence process: (a) band diagram and (b) typical glow curve.

reported that the TL response versus exposure of LiF depends on the exposure rate,[6] whereas the response of $CaF_2$:Mn and $Li_2B_4O_7$:Mn is independent of rate.[1]

---

[1]F. H. Attix, *Dosimetry for the Aurora Facility, Final Report*, Naval Research Laboratory, Washington, DC, NRL Memorandum Report 2552, Revised (March 1973).

[6]N. Goldstein, *Dose-Rate Dependence of Lithium Fluoride for Exposures above 15,000 R per Pulse*, Health Physics, 22 (1972), 90.
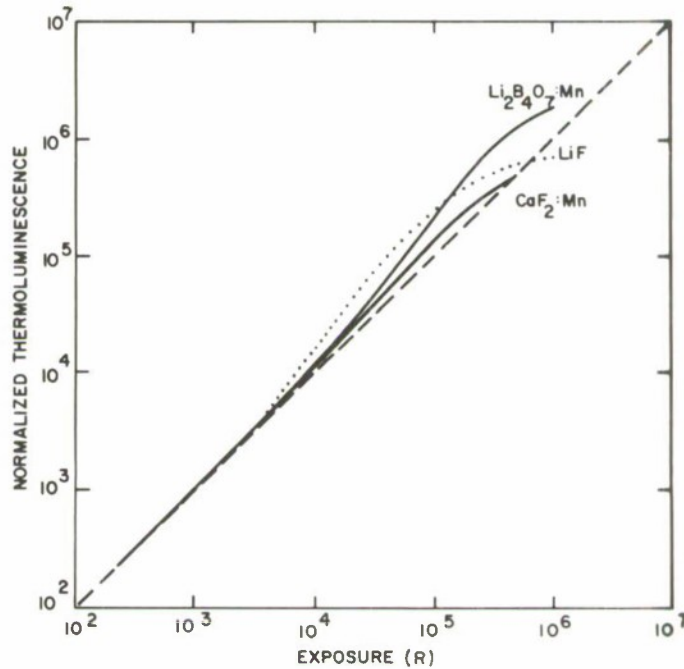
Figure 3.   Thermoluminescence response versus exposure of
            three phosphors.


Most experimenters at AURORA are interested in having the dose
measured in units of rads(Si).  The dose in silicon, with the dose known
in some material, X, is given by

$$D_{Si} = \frac{\left(\mu_{en}(E)/\rho\right)_{Si}}{\left(\mu_{en}(E)/\rho\right)_{x}} \, D_x \tag{12}$$

where $\mu_{en}(E)/\rho$ is the mass energy absorption coefficient for the
indicated material at photon energy E.  If the photons are not
monoenergetic, and if the photon energy spectrum $d\phi(E)/dE$, [MeV/MeV-sr],
is known, the conversion becomes

$$D_{Si} = \frac{\left[\int \frac{d\phi(E)}{dE} \, \frac{\mu_{en}(E)}{\rho} \, dE\right]_{Si}}{\left[\int \frac{d\phi(E)}{dE} \, \frac{\mu_{en}(E)}{\rho} \, dE\right]_{x}} \, D_x \; . \tag{13}$$

13

If the spectrum, $\phi(E)$, is known only approximately, as is usually true, the dose conversion can be calculated only approximately.

The mass energy absorption coefficients for Si and $CaF_2$:Mn are almost identical over the range 300 keV < E < 10 MeV (fig. 4). The ratio of equation (12) is constant at 0.99 over the same range. Equation (12) then becomes

$$D_{Si} \cong 0.99\ D_{CaF_2:Mn} \tag{14}$$

and this relationship is independent of photon energy over the given energy range. The practical consequence of this is that $CaF_2$:Mn dosimeters can be used to measure silicon dose with no need for detailed knowledge of the photon energy or spectrum.

Finally, a secondary advantage of $CaF_2$:Mn is that its thermoluminescence response has only one relatively high temperature glow peak, so that no preread annealing steps are required to achieve reproducible results.
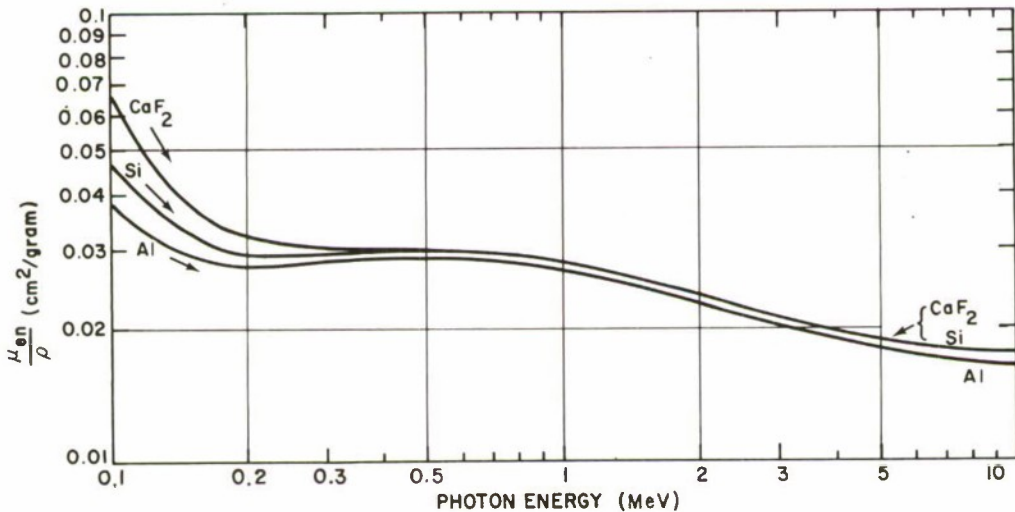


Figure 4. $\mu_{en}/\rho$ for Si, Al, and $CaF_2$:Mn.

Nonlinearity of $CaF_2$:Mn.--Earlier references to $CaF_2$:Mn have generally reported its thermoluminescence response to be linear with exposure from 1 R to about $2 \times 10^5$ R.[3] However, in the process of choosing a dosimeter for use at AURORA, it was discovered that $CaF_2$:Mn is indeed not linear for exposures above $10^3$ R (fig. 5). The differences in the nonlinearity curves for the various forms of $CaF_2$:Mn dosimeters are attributed to a combination of an actual supralinearity of light output that is the same for all three dosimeters, with a dose dependent darkening of the material causing varying degrees of light self-absorption.

If the TL response of $CaF_2$:Mn had been truly a linear function of dose, it would have been possible to adjust a TL analyzer so that its output (i.e., light-sum response) was numerically equal to the dose. The consequences of having to apply a dose-dependent nonlinearity correction to all readings are discussed fully in section 6 on data reduction.
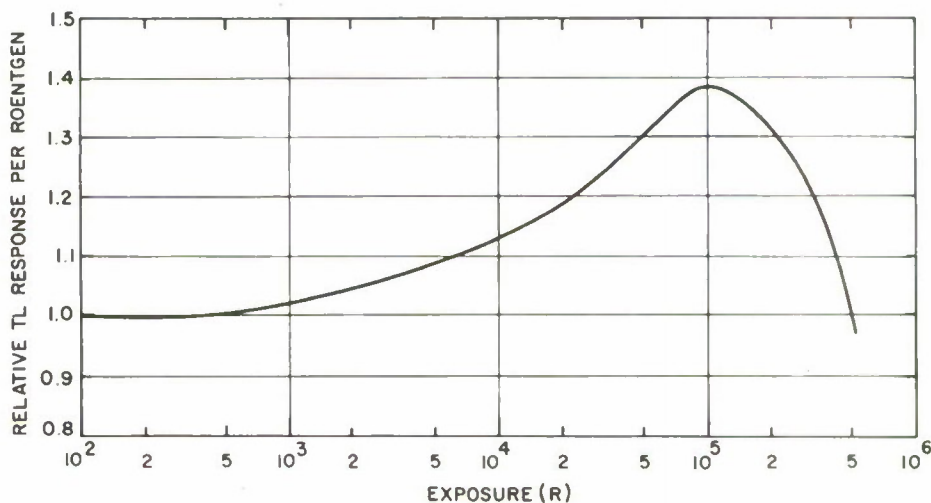


Figure 5. Thermoluminescence light-sum response per roentgen for $CaF_2$:Mn (from S. G. Gorbics, F. H. Attix, and K. Kerris, Health Physics, 25 (1973), 499).

Fading of $CaF_2$:Mn.--A second property of $CaF_2$:Mn that has an important effect on data analysis is that the light output for a given dose is not independent of the elapsed time between irradiation and readout. This fading of the TL response is shown in figure 6.

---

[3] F. H. Attix, W. C. Roesch, and E. Tochilin, Radiation Dosimetry, 2nd Ed., Academic Press, New York (1966).
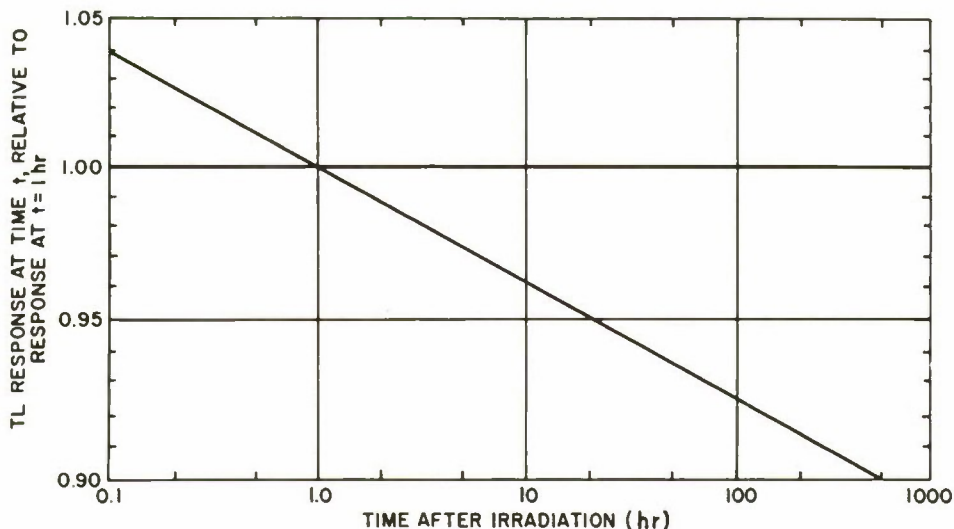
Figure 6.  Fading of the thermoluminescence response of $CaF_2$:Mn.


If $y_0$ is the light-sum response of the TLD when read at time $t_0$ after irradiation, then  the  light-sum response at other times is quite well represented by[2],*

$$ y = y_0 \left( t/t_0 \right)^{-0.017} . \tag{15} $$

Since the elapsed time t varies over  a  number of hours or days when a large  number  of  TLD's  is  exposed  on  a single  shot,  this  fading correction cannot be ignored, but must be included in the data.

CaF₂:Mn TL phosphor is commercially available in three forms:

(a) 80-200 mesh powder[†] [‡]

(b) 0.125 × 0.125 × 0.035 in. hot-pressed blocks [‡]

(c) 6-mm diam, 0.4-mm-thick discs  of  Teflon  intimately mixed with finely powdered $CaF_2$:Mn.[†]

---

[2] S. G. Gorbics, F. H. Attix, and K. Kerris, Thermoluminescent Dosimeters for High-Dose Applications, Health Physics, 25 (1973), 499.
*Reference 2 gives $y/y_0 = 1 - 0.017 \ln\left( t/t_0 \right)$. Equation (15) represents the data equally well.

The decision on which one to use for routine dosimetry at AURORA was based principally on matters of convenience and cost. The detailed tradeoffs[1] are summarized below.

Powder had the lowest price per dosimeter (10¢), assuming 10-mg samples and no reuse of the powder, but its use was considered impractical because of the time involved in measuring out and encapsulating uniform 10-mg samples of powder. It is also very difficult to envision an automatic sample changer for a TLD reader that could handle powder samples.

Hot-pressed blocks had the highest unit price ($1.75), requiring their being annealed and reused repeatedly. They can be if they are never irradiated above 50 to 100 rads(Si). However, at higher doses, their calibration changes after several irradiation and annealing cycles, making this mode of operation impractical.

The Teflon discs were priced low enough (30¢) to permit their being used once only. They are easy to handle and adaptable to automated loading. Finally, the sample-to-sample reproducibility for TLD's from the same production lot was ±3.1 percent (1 σ), which is acceptable for routine use at AURORA. The sample-to-sample reproducibility gets quite a bit worse around 10 rads(Si), so that these TLD's are not used for measuring doses below 50 rads(Si).

The following TLD's were adopted as standard for routine use at AURORA:

(a) For $50 \leq D \leq 10^5$ rads(Si): Teflon disc containing 5 percent by weight $CaF_2:Mn$; Teledyne Isotopes SD-$CaF_2$:Mn-0.4L. These TLD's are procured in quantities of 15,000 from the same production lot.

(b) For mrad(Si) $\leq D \leq$ 50 rads(Si): Harshaw Chemical Company, 0.125 × 0.125 × 0.035 in. hot-pressed $CaF_2$:Mn blocks. One thousand were procured from the same production lot. It is not known how often these can be irradiated, annealed, and reused before the individual calibrations drift enough to make a batch calibration invalid. At very low doses ($D \leq 1$ rad(Si)), dry nitrogen gas flow must be used with these TLD's during the readout cycle to suppress spurious luminescence caused by absorbed oxygen.

---

[1] F. H. Attix, *Dosimetry for the Aurora Facility, Final Report, Naval Research Laboratory, Washington, DC, NRL Memorandum Report 2552, Revised (March 1973).*

## 4. TYPES OF MEASUREMENT

These TLD's can be used to make two entirely different kinds of silicon dose measurements, and it is very important to understand the distinction between them.

Assume that an experimenter is irradiating a large, complex electronic system at AURORA. Somewhere inside this system in some critical circuit is a silicon transistor or integrated circuit, and the experimenter wants to know the dose absorbed by this component in rads(Si). The active volume of silicon is very small compared to the rest of the system, so that all the energy deposited in this volume of silicon comes from secondary electrons produced by photons somewhere in the surrounding hardware, and none comes from primary photon interactions in the silicon itself.

The way to determine this dose is to put a small dosimeter very near this critical component. It will then see very nearly the same secondary electron environment as the transistor, and the dose absorbed by the TLD will be related to the transistor dose by the ratio of the two electron stopping powers. Since the dosimeter has a stopping power almost identical to that of silicon over a wide range of electron energies, this ratio is nearly one, and it is constant over a large energy range, making the measurement largely independent of any detailed knowledge of the AURORA bremsstrahlung spectrum.

So to measure the local silicon dose inside a nonuniform, rather lumpy system, a bare $CaF_2$:Mn TLD is placed as closely as possible to the exact point of interest. This kind of measurement is normally called Type-A at AURORA.

However, assume that this is not the measurement the experimenter wants. Rather, he wants to know the photon fluence incident on his system in rads(Si). Of course, photon fluence is not measured in rads(Si) but $MeV/cm^2$ as a function of photon energy. So what does rads(Si) incident mean? It means, simply, the dose that would be deposited in silicon under conditions of CPE by the incident fluence, whatever it may be. The actual fluence as a function of photon energy would be a very difficult measurement, but the equilibrium silicon dose is easy. One simply surrounds a silicon dosimeter with enough silicon to produce CPE. In actual practice, one uses a $CaF_2$:Mn TLD and surrounds it with aluminum. Doing so requires making a photon absorption correction for the aluminum and a stopping power correction for the $CaF_2$, but these corrections are very nearly unity and constant for 300 keV $\leq$ h$\nu$ $\leq$ 10 MeV, so that this procedure is completely valid and independent of any detailed knowledge of the AURORA spectrum.

How much aluminum is required to guarantee CPE? This question was answered experimentally by determining the dose absorbed by the TLD as a function of aluminum thickness[1] (fig. 7). The initial, rather sharp rise shows that in this region, more electrons are scattered out of the center of the aluminum capsule than are scattered into it from the walls. The secondary electron flux is low because there is no CPE. Charged particle equilibrium exists for all points to the right of the peak, but the dose slowly decreases because of attenuation of the photons by the aluminum. The optimum aluminum thickness to assure CPE without introducing attenuation is seen to be 1 gram/cm$^2$, or 0.146 in.

So, to measure the silicon equilibrium dose in the free field, one surrounds the TLD with an aluminum capsule of 5/32 in. (0.156 in.) wall thickness. This type of measurement is normally referred to at AURORA as Type-B. Figure 8 is an engineering sketch of the standard AURORA Type-B capsule.

A third kind of measurement that is sometimes requested by AURORA experimenters is the tantalum equilibrium dose, rads(Ta). This dose is measured by a small tantalum dosimeter surrounded by an equilibrium
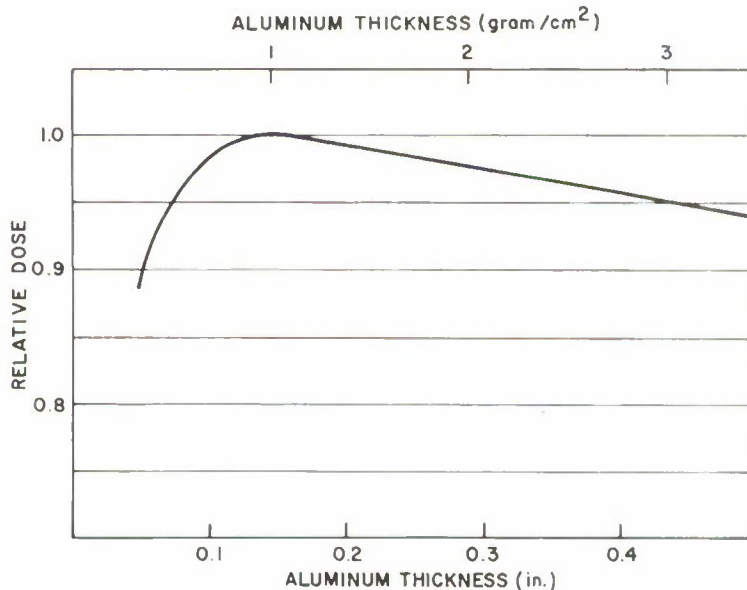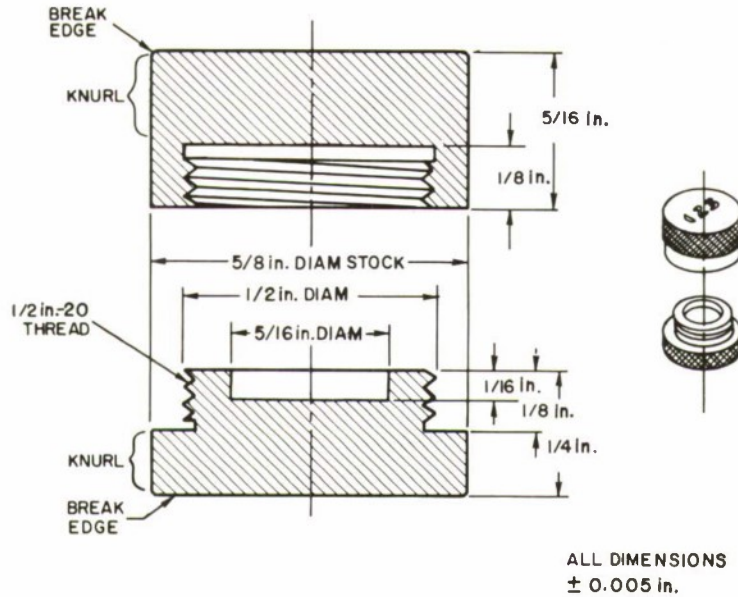


Figure 7.   Aluminum depth dose (F. H. Attix, NRL Memorandum
            Report 2552 (March 1973)).

[1]F. H. Attix, Dosimetry for the Aurora Facility, Final Report, Naval Research Laboratory, Washington, DC, NRL Memorandum Report 2552, Revised (March 1973).

**BREAK EDGE**

**KNURL**

5/16 in.

1/8 in.

5/8 in. DIAM STOCK

1/2 in.-20 THREAD

1/2 in. DIAM

5/16 in. DIAM

1/16 in.

1/8 in.

1/4 in.

KNURL

BREAK EDGE

ALL DIMENSIONS
± 0.005 in.

MAKE FROM 5/8 in. OD ALUMINUM ROD STOCK, ALLOY 6061-T6
HARD ANODIZE ALL PIECES, DYE BLUE

Figure 8.   Standard Type-B dosimeter capsule.

thickness of tantalum.  Unfortunately, at the present time, there are no high-Z TLD phosphors that approximate the electron stopping power of tantalum.  In principle, it would be possible to use a $CaF_2$ TLD with an equilibrium shield of tantalum and to make a stopping power correction for the $CaF_2$.  Unfortunately, the $CaF_2$ TLD is not sufficiently small compared with the tantalum shield for simple Bragg-Gray cavity theory[3] to apply.  What is done at AURORA is to calibrate the tantalum-clad TLD's against a tantalum calorimeter.

The tantalum capsules are formed from a 0.015-in.-thick tantalum sheet.  This configuration is called Type-C.  Figure 9 (p. 21) shows both the Teflon disc $CaF_2$:Mn TLD's and the solid $CaF_2$:Mn blocks in their Types A, B, and C configurations.  Type-C TLD capsules are 7/16 in. square by 1/16 in. thick.

5.  INSTRUMENTATION

5.1  Dose Measurement

Apparatus for reading out TLD's typically consist of a heating element, circuitry that provides a reproducible temperature cycle, and a photomultiplier tube and amplifiers to detect the light emitted during

[3]F. H. Attix, W. C. Roesch, and E. Tochilin, Radiation Dosimetry, 2nd Ed., Academic Press, New York (1966).
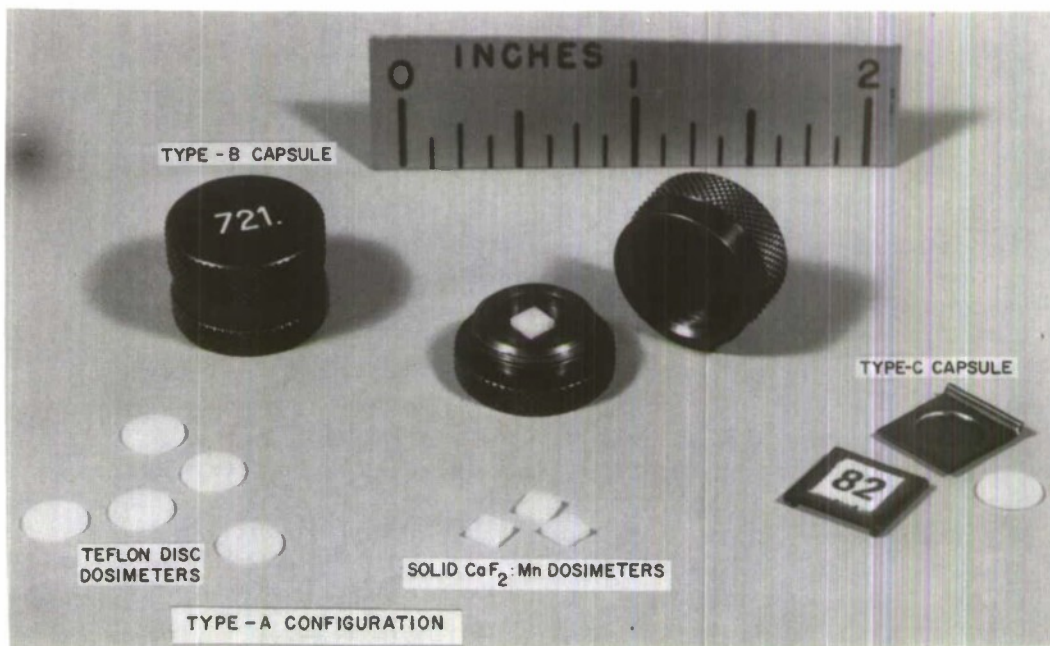
Figure 9.    Types A, B, and C dosimeter configurations.

the temperature cycle.   The heating element is usually a  small, shallow
dish  made  of some suitable material such as Monel Metal, Nichrome,  or
platinum,  which  is  heated  when  current  is  passed  through  it.
Temperature cycling can  be  accomplished  by a programmed power supply,
often with temperature  feedback from a thermocouple in contact with the
heating element.

        The  light  detecting circuitry generally includes a filter  to
block infrared radiation, a visible light filter  to  select  the proper
spectral band  for  the  phosphor  in use, a photomultiplier tube, and a
stable high voltage  power  supply.   One  most generally determines the
sensitivity of the reader by adjusting the photomultiplier voltage.   The
photomultiplier current can be amplified  and  recorded on a strip-chart
recorder to show the glow curve  or  integrated  electronically.  Either
the peak of the glow curve or  the  integral under the curve can be used
as a measure of the dose absorbed by the TL material.

        The  primary  criteria  for  the  design  of  the  readout
instrumentation  to  be used at AURORA were operational simplicity and a
high degree of  automation.   In  particular,  all  steps  requiring the
operator to copy  data  manually  were to be eliminated, with everything
being designed for eventual fully automatic  hands-off operation.   These
criteria were imposed because of  the large volume of dosimetry readings

21

required by many AURORA users.  During a large systems test, which might last for several weeks, one person is kept busy all day just reading TLD's.  It was therefore considered quite important to design the equipment to reduce operator fatigue as much as possible and to eliminate those steps in which operator fatigue might introduce errors into the data.

A secondary requirement on the TLD readout  instrumentation was that it be flexible enough to accommodate the large variety of TL materials required for specialized measurements.  Although $CaF_2$:Mn is the most commonly used phosphor at AURORA, it was thought  possible that LiF, $CaSO_4$, $Li_2B_4O_7$, and other phosphors would be used for some applications.

The instrument chosen for use at AURORA was the Harshaw Model 2000 Thermoluminescence Analyzer.  It has a very versatile temperature cycle programmer and linear and logarithmic glow-curve outputs;  these fully satisfy the flexibility criterion.  The integral under the glow curve (light sum) is displayed digitally and is also available in digital form at a rear panel connector, making it possible to achieve semiautomated or fully automatic operation.

The most likely chance for operator error in making many repetitive measurements is in miscopying the data.  Therefore the first step toward automating the readout process was to add a printer to print the light sum of each measurement automatically.  The Harshaw TLD reader furnishes a print command at its rear panel connector at the end of each readout cycle, so that the printer connection is easily made.  The printer used for this purpose is a Systron-Donner Model 5103 20-column printer.

The sensitivity of the TLD reader is adjusted so that the value of the light sum as  printed on the paper tape is approximately equal to the dose in rads(Si), except for a factor equal to a power of 10.  Since the dose response of $CaF_2$:Mn is not exactly linear, the printer output can be made equal to the dose only at one particular dose.  In practice, the calibration is chosen to give a one-to-one correspondence at a dose of about 20 krads(Si), because TLD's are most frequently used to measure doses from 5 to 40 krads(Si) at AURORA.

Another difficulty was finding a way to print the proper multiplier (i.e., power of 10) for the printed data.  On its lowest range, the TLD reader rear panel output consists of four digits, with the least significant digit equal to 1 pC.  The display automatically ranges up by factors of 100; that is, when the display reaches 9999 pC, the addition of one more picocoulomb results in 0100 (×100) pC, and so on up through three range changes.  The proper range is automatically indicated on the front panel by a shifting decimal point and illuminated

nanocoulomb and microcoulomb indicators. However, at the rear panel connector, the range in use is indicated by a two-digit binary number, $00_2$ signifying the lowest range (1 digit = 1 pC) and $11_2$ indicating the highest (1 digit = 1 μC). Further, the basic calibration of the reader can be 1, 10, or 100 rads(Si)/nC.

This problem was solved by constructing an interface circuit that does two things. First, it puts a constant decimal point between the most significant and next most significant digits printed on the paper tape, thus: X.XXX. Secondly, it accepts the two-digit range code from the Harshaw reader and a two-digit code (programmed by toggle switches) indicating the basic reader sensitivity. It decodes this input and commands the printer to print a fifth digit representing the correct exponent for the power-of-10 multiple to be applied to the data. For example, a printout of 1.234 5 R is to be interpreted as $1.234 \times 10^5$ rads(Si), except for nonlinearity and fading corrections.

The truth table for these decoding operations is given in table I. An example may illustrate how this works. Suppose a reader with a basic calibration of 10 rads(Si)/nC indicates a light sum of 03.22 μC on its front panel display. The printer output will be 0322 and the range indication, $10_2$. For a toggle switch setting of $01_2$, the decoded exponent of 10 will be 5, and the printer will print 0.322 5 R ($0.322 \times 10^5$ rads(Si)).

(Verify: 10 rads(Si)/nC $\times 3.22 \times 10^3$ nC = $3.22 \times 10^4$ rads(Si)).

TABLE I.  RANGE DECODING TRUTH TABLE

| Harshaw range data[a] | Reader calibration toggle switch setting | | | |
| | $00_2$ (1 rad(Si)/nC) | $01_2$ (10 rads(Si)/nC) | $10_2$ (100 rads(Si)/nC) | $11_2$ (1000 rads(Si)/nC) |
| --- | --- | --- | --- | --- |
| | Decoded exponent | | | |
| $00_2$ (LSD[b] = 1 pC) | 0 | 1 | 2 | 3 |
| $01_2$ (LSD = 100 pC) | 2 | 3 | 4 | 5 |
| $10_2$ (LSD = 10 nC) | 4 | 5 | 6 | 7 |
| $11_2$ (LSD = 1 μC) | 6 | 7 | (c) | – |

[a] Subscript 2 = base - 2 (binary) numbers.
[b] LSD = least significant digit.
[c] = no code.

The decoding circuit is easily implemented with an SN74154 4- to 16-line decoder and three SN7430 eight-input NAND gates (fig. 10). Two toggle switches furnish either a logic 0 or 1 at the A and B inputs. The Harshaw range output is connected to the C and D inputs. The output to the printer is binary-coded decimal (BCD), with the most significant bit hardwired to logic 0. The BCD output of the circuit of figure 10 follows the truth table of table I.

To identify the numbers on a long strip of printer tape with specific dosimeters, a provision to print a three-digit identifying number along with each dose datum was incorporated into the interface unit. This identifying number is input via a 10-key keyboard and printed at the extreme left of the paper strip; so a datum of

> 357          0.322 5 R

means that the dose (uncorrected) of $3.22 \times 10^4$ rads(Si) is to be identified with TLD number 357. The identifying number can be keyed in two modes, selected by a toggle switch. In the MANUAL mode, used when there are few TLD's or the identification numbers are in some random order, the number register is cleared after each print cycle, and a new number must be keyed in for each reading. If there are many readings in
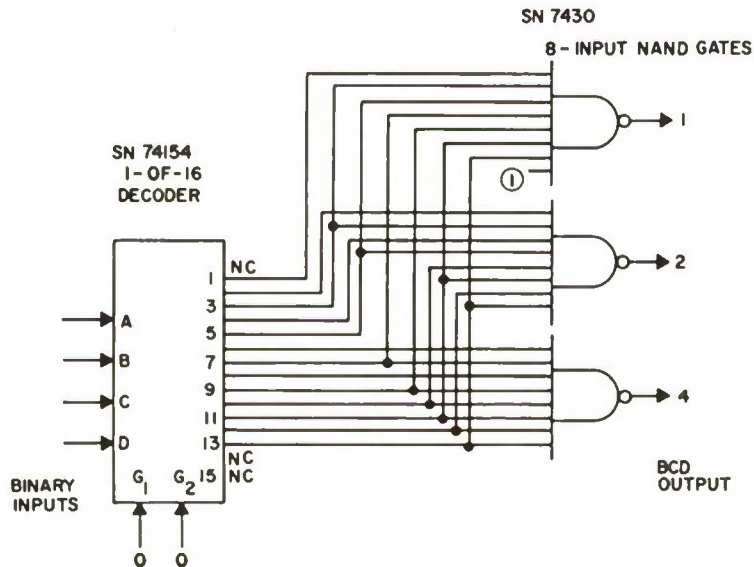


Figure 10.   Range decoding circuit.

24

numerical sequence, an AUTOMATIC mode is provided.  In  this mode, only the  first  number  need  be  keyed  in;  the  identifying  number  is automatically increased by  one every time a reading is made and another READ cycle is initiated.  This increase is made possible by a READ level change  being available at the  rear  panel  connector  of  the  Harshaw reader.  A light-emitting diode display on  the  interface unit displays the identifying number and the exponent of 10.

The  TLD  identifying  number  circuit  is  shown in figure 11. Whenever a digit key is pressed, the BCD data appear  at  the data input of all three SN74192 asynchronous BCD up-down counters.  If this is  the first  key  that  is  pressed, the address shift register applies a load enable pulse  to  the counter for the most significant digit (MSD).  The second time a key is pressed, the second digit is enabled, and the third keystroke enables the least significant digit (LSD).  The outputs of the counters are connected to the  first three columns of the printer.  Upon completion of a PRINT cycle,  the  digital  printer sends a pulse to the mode control  circuitry.  If the switch is in the MANUAL position, this pulse clears the BCD counters and resets the address shift register.  If the switch is in the AUTOMATIC position, the RESET pulse is blocked, and the next succeeding READ cycle  initiation  causes  a  COUNT pulse to be applied to the LSD counter.
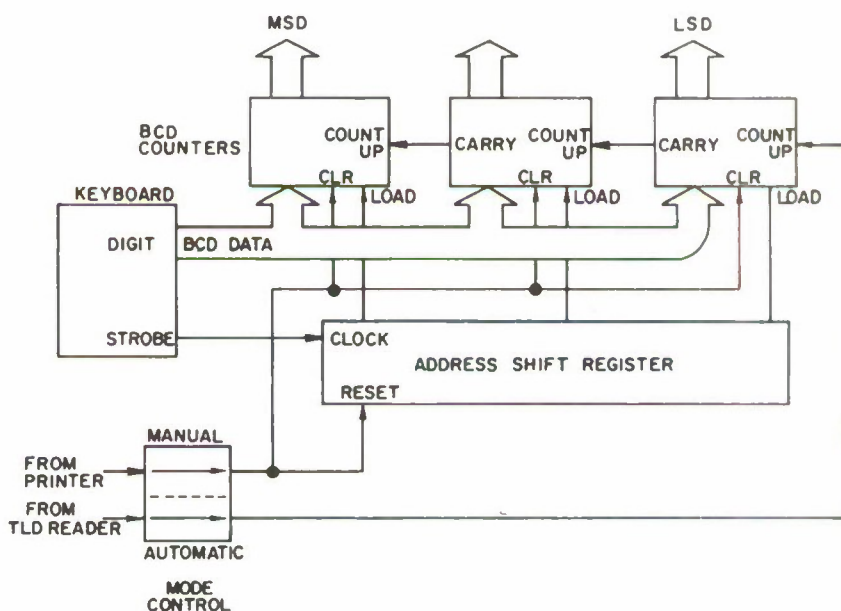


Figure 11.  Dosimeter identifying number circuit.

25

The address shift register consists of two SN7474 dual-D flip-flops, one SN7400 quad two-input NAND gate, and two SN74121 one-shots. The mode control circuit contains two SN74121 one-shots. The entire interface unit circuit is shown in figure 12. LOAD ENABLE pulses are triggered by the leading edge of the keyboard STROBE pulse; the SHIFT REGISTER CLOCK pulse is derived from the trailing edge of this STROBE pulse. RESET and CLEAR pulses are generated by the trailing edge of either the keyboard CLEAR KEY pulse or the printer +INHIBIT pulse. The COUNT UP one-shot puts out a 1-s pulse to suppress multiple pulsing by a very bouncy READ switch on the Harshaw reader. The mode is controlled by switching the logic levels of appropriate inputs on the RESET and COUNT UP one-shots.

Figure 13 shows the entire TLD reader system. The only manual operations required are opening the sample drawer, inserting a TLD, closing the sample drawer, and pressing the READ button. Data recording is automatic, eliminating the possibility of erroneous data entry by hand. A portion of a sample data tape is shown below.

```
018   04   1459   1   .666   4   R
017   04   1457   1   .596   4   R
016   04   1445   1   .505   4   R
015   04   1444   1   .664   4   R
014   04   1443   1   .599   4   R
013   04   1441   1   .715   4   R
012   04   1440   1   .497   4   R
011   04   1439   1   .634   4   R
```

The first number is the TLD identifying number. The next two numbers are the day of the month and 24-hr time of the reading. This information is necessary for calculation of the fading correction for $CaF_2$:Mn TLD's. This information is generated by an Option D102-H clock board inside each printer. The final numbers represent the dose in approximate rads(Si).

It is tempting to imagine a fully automatic system, including some sort of mechanical TLD changing device that would eliminate the steps of drawer opening and closing and button pushing. Such a device is now under construction. When complete, it will accept a magazine of up to 200 TLD's, read them, and record the data, all automatically. Since each complete readout cycle takes 90 s, each automatic readout of one 200-TLD magazine would represent a savings of 5 man-hours.

26

Figure 12. Interface unit circuit.

27
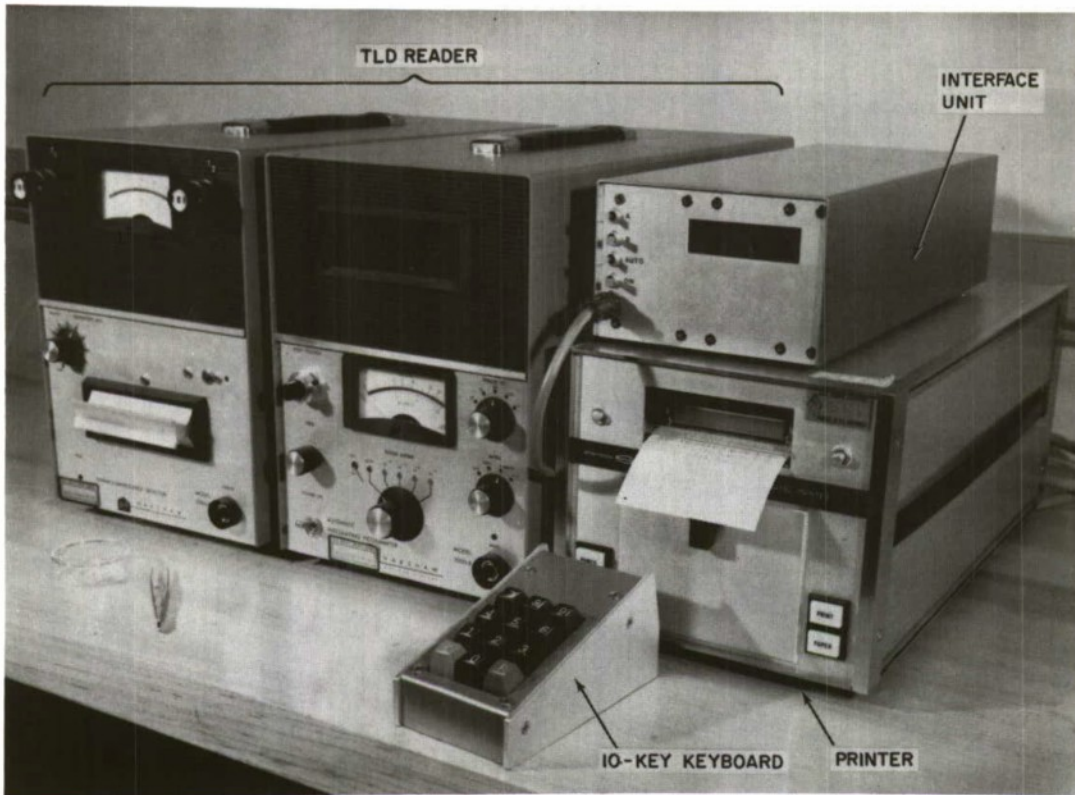
Figure 13. Thermoluminescent dosimeter reader, printer, and interface unit.

## 5.2 Dose Rate Measurement

The AURORA bremsstrahlung pulse is measured on every shot by use of a scintillator-photodiode combination. The detector is usually placed so that the scintillator is as near the experimenter's cassette and the machine center line as feasible. The light from the scintillator is coupled to the photodiode by a hollow aluminum light pipe 4- or 6-ft long. The photodiode is usually placed near the floor of the test cell, inside a 4-in. thick lead shield. This arrangement is diagrammed in figure 14.

The scintillator is usually Pilot-B, either a cylinder 3 in. diam × 3 in. long or a disc 3 in. diam × 1/16 in. thick, depending on the dose rate. When it is desired to look at very high dose rates
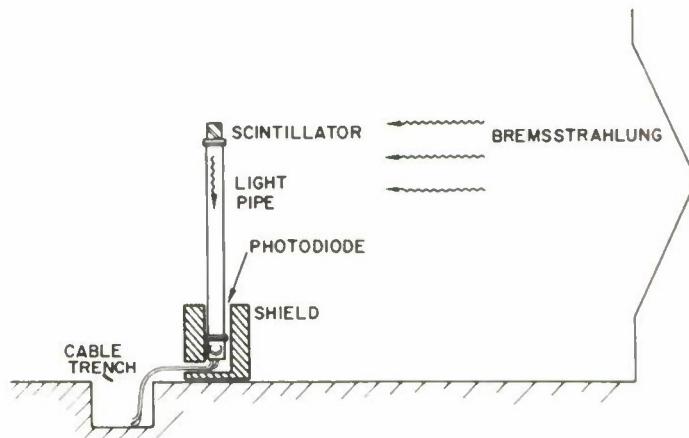
28

Figure 14. Scintillator-photodiode detector setup.

($>5 \times 10^{10}$ rads(Si)/s), the Cerenkov radiation from a cylinder of lucite 3 in. diam × 3 in. long is detected.[7]

The photodiode detector is powered by a 5-kV power supply, and its output signal, properly attenuated, is displayed by one or more Tektronix 519 oscilloscopes. The circuit for the photodiode detector is shown in figure 15.[8]
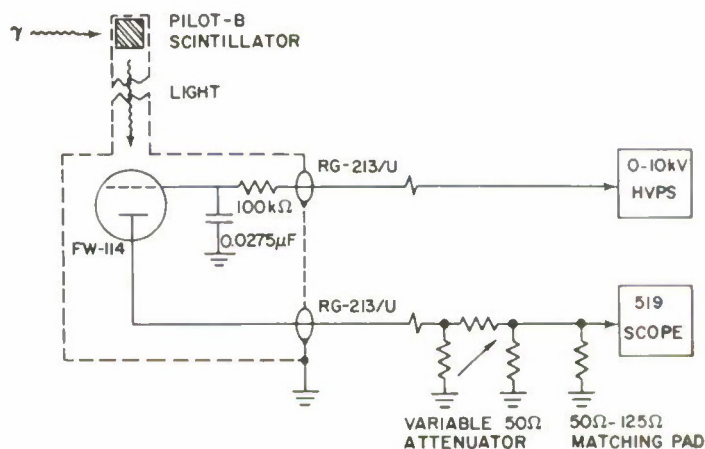


Figure 15. Detector circuit.

[7]J. E. Doyle and W. C. Dickinson, The Cerenkov Response of Lucite and Quartz to Gamma and Fast Neutron Radiation, University of California Lawrence Radiation Laboratory, UCRL-7032 (TID4500) (July 1962).

[8]R. K. Durkee, Design and Test of a Modular Scintillation Detector System, EG&G, Santa Barbara Division, Technical Report S-466-R (March 1970).

The detector is not normally calibrated. The dose rate at each spatial point of interest is determined by measuring the dose at that point with a TLD, assuming that the pulse shape at that point is the same as that at the Pilot-B scintillator. The dose rate is then calculated from the known dose and pulse shape.

## 6. DATA ANALYSIS

The number printed by the digital printer is proportional to the light-sum output of the TLD. As such, the number is not very useful, since the light sum (for the Teflon disc TLD's) is a nonlinear function of the dose. In addition, the light sum fades with time. If the light sum were a linear function of dose, and if all TLD's were always read at the same time relative to irradiation, the printed number could always be made equal to the dose by appropriate adjustment of reader sensitivity (via the photo-tube high voltage) and interface unit decoder switch settings.

As things stand, however, the printed number, P, must be corrected by multiplying by a nonlinearity correction, $K_L$, and a fading correction, $K_F$. The nonlinearity correction is a function of the dose, and the fading correction is a function of the time elapsed between irradiation and reading.

### 6.1 Nonlinearity Correction

We define the following quantities,

   y = light-sum output of TLD

   X = exposure, roentgens

   $D_{Si}$ = dose, rads(Si)

   P = TLD reader printout.

We are looking for a nonlinearity correction factor, $K_L$, such that

$$D_{Si} = K_L(P) \times P \ . \tag{16}$$

Figure 5 shows the relative thermoluminescence, $y(X)/y(X_0)$, per roentgen, as a function of the $Co^{60}$ exposure, X. This nonlinearity

30

curve was determined by irradiating a number of TLD's to various exposures, X, and determining the corresponding values of $y(X)$. To find $K_L(P)$, use the data in figure 5, but plot $Xy(X_0)/y(X)$ as a function of $y(X)$. Now, $P(X)$ is proportional to $y(X)$, so $P(X) = Cy(X)$. Also, $D_{Si}(AURORA) = 0.870X(Co^{60})$. Applying these two relationships gives a new plot of $D_{Si}/P(D)$ as a function of $P$. But the constant of proportionality, $C$, between the light-sum response and the printout is arbitrary, depending on the sensitivity setting of the TLD reader.

To make the printed data, $P$, nearly equal to $D_{Si}$ for most cases of practical interest at AURORA, choose $C$ such that $K_L = D_{Si}/P = 1.000$ for $P = 1.55 \times 10^4$. The resulting curve of $K_L$ versus $P$ is given in figure 16. This is our standard nonlinearity correction curve. When $P = 1.55 \times 10^4$, $D_{Si} = 1.55 \times 10^4$ rads(Si). All other readings, $P$, must be multiplied by $K_L$ to find the dose. For instance, if $P = 3.0 \times 10^3$ for a given dosimeter,

$$D_{Si} = K_L(P) \times P = 1.11 \times 3 \times 10^3 = 3.33 \times 10^3 \text{ rads(Si)}.$$
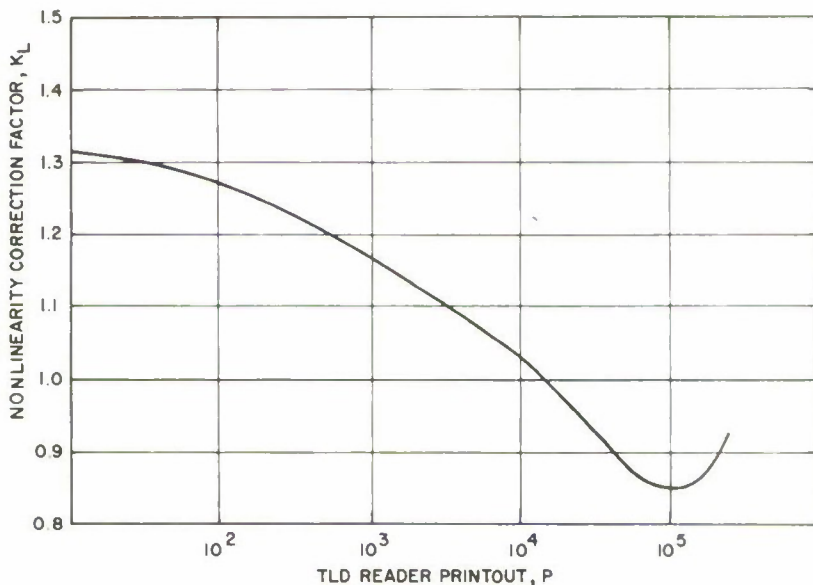


Figure 16. Standard nonlinearity correction for Teledyne-Isotopes SD-CaF$_2$:Mn-0.4L.

This can be calculated by hand with figure 16. However, for many values of P, hand calculation becomes excessively laborious. For machine calculation, it would be very desirable to have an analytic expression of $K_L$ as a function of P. The expression was found by least-squares fitting a fifth-degree polynomial to the data of figure 16. That is, represent $K_L$ by

$$K_L(P) = \sum_{n=0}^{5} a_n (\log P)^n \tag{17}$$

where the coefficients $a_0$ to $a_5$ are found to be

$$
\begin{aligned}
a_0 &= 0.99635 \\
a_1 &= 0.76943 \\
a_2 &= -0.67278 \\
a_3 &= 0.26418 \\
a_4 &= -0.050483 \\
a_5 &= 0.0036386 \ .
\end{aligned}
\tag{18}
$$

This polynomial representation deviates from figure 16 by at most 2 percent and on the average by less than 1 percent. Given a value, P, the silicon dose, $D_{Si}$, is given by

$$D_{Si} = P \sum_{n=0}^{5} a_n (\log P)^n \tag{19}$$

where $a_0$ to $a_5$ are given by equations (18).

## 6.2 Fading Correction

The analytical expression for the fading of the light-sum response was given in equation (15) by

$$y = y_0 \left(t/t_0\right)^{-0.017}.$$

32

But P is proportional to y, so

$$P = P_0 \left( t/t_0 \right)^{-0.017} .$$ 
(20)

The reader is calibrated to give the correct dose when the TLD is read exactly 1 hr after irradiation. So the P to be used in equation (19) is $P_0$, which is related to the actual P by

$$P_0 = P \left( t/t_0 \right)^{+0.017} .$$ 
(21)

Combining the nonlinearity correction equation (19) with the fading correction equation (21) and setting $t_0 = 1$ hr gives the final expression for the silicon dose absorbed by a TLD, which gives a reading P when read at a time t hours after irradiation

$$D_{Si} = P\, t^{0.017} \sum_{n=0}^{5} a_n (\log P)^n .$$ 
(22)

## 6.3 Solid CaF$_2$:Mn TLD's

The response for these TLD's is almost linear with dose, at least over the range of 0 to 200 rads(Si). However, the fading correction must still be made, as for the Teflon discs. Using a $Co^{60}$ calibration technique exactly as described for the Teflon disc TLD's, and with the TLD readers calibrated so that equation (22) is true, one can find the analogous equation for solid CaF$_2$:Mn TLD's

$$D_{Si} = \sum_{n=0}^{2} b_n (P\, t^{0.017})^n$$ 
(23)

where $b_0$ through $b_2$ are found by fitting a quadratic equation to the calibration curve by the method of least squares.

## 6.4 Dose Rate Calculation

The dose rate is found from the dose, by use of the known pulse shape of the radiation pulse as determined by the scintillator-photodiode detector. The area under the pulse is found by numeric integration. Dividing the area by the peak height gives the effective pulse width. "Effective" pulse width means the width of a

33

rectangular pulse having the same area and the same peak height as has the AURORA pulse. Since the dose is proportional to the area under the AURORA pulse, the dose divided by the effective width equals the dose rate at the peak of the pulse:

$$\text{dose rate at peak} = \frac{D_{Si}}{t_{eff}} \text{ (rads(Si)/s)} \tag{24}$$

where

$$t_{eff} = \frac{\text{area under pulse}}{\text{peak height}} . \tag{25}$$

## 6.5 Calculation of Data

The calculations required for equations (22) to (25) appear to be quite involved; however, they are simply implemented in practice. All calculations are done on the Hewlett-Packard 9820A programmable desk calculator equipped with a 9861A typewriter, 9862A plotter, and 9864A digitizer.

The oscilloscope trace representing the photodiode pulse is traced with the digitizer cursor. The calculator computes the peak height and the area, using the trapezoidal rule, while the plotter draws an enlarged picture of the pulse on the data sheet. The operator then places the data sheet in the typewriter. He enters the shot number, time of irradiation, time of reading (column 2 of the data tape), and first and last TLD identification numbers (column 1 of the data tape). He then enters the raw data, P (column 3 of the data tape), in sequence. The calculator calculates the elapsed time, dose, and dose rate by equations (22) to (25) and causes the typewriter to type all data on the data sheet.

Figure 17 reproduces a typical data sheet. Note the picture of the pulse to the scale of 100 ns/in., pulse parameters, and dose and dose rate data. The raw data used to produce this data sheet are like those shown on the sample data tape in section 5. The raw data, P, are approximately equal to the doses, permitting preliminary data evaluation as the TLD's are read.

This data reduction system using the Hewlett-Packard Model 20 programmable desk calculator can be easily adapted to fully automated data taking. In this case, the raw data, P, would not be manually punched into the calculator, but it would be directly coupled in from

34

DOSIMETRY DATA for Shot 1737
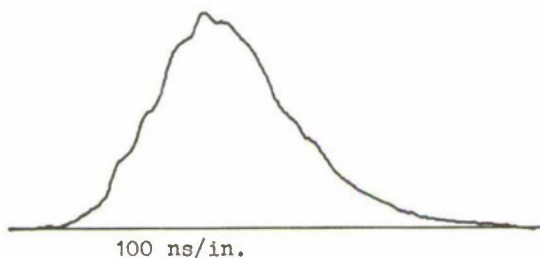
Date:     4 Mar 75

Zero time:   1100

Area:   194 in.-ns

Peak Height: 1.59 in.

Eff. Width:   122 ns

100 ns/in.

| Dosimeter No. | DOSE (rads(Si)) | DOSE RATE at peak (rads(Si)/s) |
|---|---|---|
| 11 | 1.632E 04 | 1.339E 11 |
| 12 | 1.507E 04 | 1.236E 11 |
| 13 | 1.705E 04 | 1.399E 11 |
| 14 | 1.600E 04 | 1.312E 11 |
| 15 | 1.659E 04 | 1.361E 11 |
| 16 | 1.514E 04 | 1.242E 11 |
| 17 | 1.597E 04 | 1.310E 11 |
| 18 | 1.661E 04 | 1.362E 11 |

Figure 17.   Example of dose and dose-rate data sheet.

the interface unit by an appropriate data coupler. Alternatively, the data could be recorded on a magnetic tape cassette and later played back into the Model 20. Such an automatic data recording system using an Electronic Processors STR-200I incremental cassette recorder, a parallel-to-serial converter, and the HP 11202A TTL I/O Interface Card is now under construction.

Combining such an automatic data reduction system with an automatic TLD changer could result in complete hands-off reading and data reduction of up to 200 TLD's at a time.


7.   CALIBRATION

Two methods are routinely used to calibrate and monitor the calibration of the AURORA TLD readers.


(a)  A number of TLD's are exposed for a fixed time interval in a $Co^{60}$ source whose exposure rate is well known. The corresponding dose deposited by AURORA radiation can be calculated and compared with the dose calculated from the TLD reader output.

(b)  A number  of  TLD's is  exposed to an AURORA pulse alongside an absolute silicon-dose calorimeter.  The silicon dose  as calculated from the reader output is  compared  with  the  dose  measured by the silicon calorimeter.

### 7.1  Cobalt-60 Calibration

The success of $Co^{60}$ calibration* depends on two things.  First, the  exposure  rate  at a  given position  in  a  $Co^{60}$ source must be accurately known.  The rate is usually determined with  air-equivalent ionization chambers calibrated by the National Bureau of Standards.  The second is the ability to convert $Co^{60}$ exposure in  roentgens  to  AURORA silicon  dose  in  rads(Si).  This ability requires a knowledge of  the AURORA spectrum, which we do not have.  However, some careful  estimates yield results that are believed to be quite good.

The  assumption  behind  this  derivation  is  that  the thermoluminescence response of  a  TLD  will  be the same for equal dose (rads($CaF_2$:Mn)), whether this dose is deposited  by  $Co^{60}$  or  by  AURORA bremsstrahlung.

First, one  calculates $D_{CaF_2}$, deposited by $Co^{60}$.  To ensure CPE one exposes the TLD  in  a  0.43-cm-thick  aluminum  capsule.  Given the unperturbed  free  field  exposure, $X_0$, in  the  $Co^{60}$ source,  the  true exposure, X, at the TLD is

$$X = X_0 \exp\left(\left(-\mu_{en}/\rho\right)\rho't\right) = 0.971X_0 \tag{26}$$

where $\mu_{en}/\rho$ is the mass energy absorption coefficient for $Co^{60}$ radiation in aluminum, and t is the aluminum thickness.

To determine $D_{CaF_2}$ from  X,  one  assumes  that the TLD in the aluminum capsule behaves like a Bragg-Gray  cavity.[3]  That  is,  primary photon interactions occur only in  the  aluminum,  and  all  of the dose deposited in the $CaF_2$ is by secondary electrons from the aluminum.[†]

---

[3]F. H. Attix,  W. C. Roesch,  and  E. Tochilin, Radiation  Dosimetry, 2nd Ed., Academic Press, New York (1966).

*F. H. Attix provided this analysis.

[†]This assumption is  not  necessarily  valid,  because  of the finite thickness of the TLD;  nevertheless,  it  is justified here, because the stopping power ratio approximately equals  the  mass  energy  absorption coefficient ratios.

From the definitions of the rad and the roentgen, we know that, for $Co^{60}$ radiation,

$$D_{air} = 0.869X . \tag{27}$$

Considering just the primary photon interactions in aluminum,

$$D_{Al} = \frac{\left(\mu_{en}/\rho\right)^{Al}{}_{Co^{60}}}{\left(\mu_{en}/\rho\right)^{air}{}_{Co^{60}}} = D_{air} = 0.966D_{air} \tag{28}$$

(values of $\mu_{en}/\rho$ are found in standard tables[3,10]). If all the dose in the $CaF_2$ comes from secondary electrons produced in the aluminum, the average energy of these secondary electrons would be approximately 300 keV. Then,

$$D_{CaF_2} = \frac{S^{CaF_2}_{300\ keV}}{S^{Al}_{300\ keV}}\ D_{Al} = 1.013D_{Al} \tag{29}$$

(values of S are found in standard tables[9,11]), where $S^{Z}_{E}$ is the electron stopping power of material Z for electrons of energy E. Combining equations (27) to (29) gives

$$D_{CaF_2} = 1.013 \times 0.966 \times 0.869X = 0.850X \tag{30}$$

for the dose deposited in $CaF_2$ by $Co^{60}$ gamma radiation.

---

[3]F. H. Attix, W. C. Roesch, and E. Tochilin, Radiation Dosimetry, 2nd Ed., Academic Press, New York (1966).

[9]Ann T. Nelms, Energy Loss and Range of Electrons and Positions, National Bureau of Standards (U.S.), Circ. 577 (1956).

[10]J. Hubbell, Photon Cross Sections, Attenuation Coefficients, and Energy Absorption Coefficients from 10 keV to 100 GeV, National Bureau of Standards NSRDS-NBS29 (August 1969).

[11]M. Berger and S. Seltzer, Tables of Energy Losses and Ranges of Electrons and Positrons, National Aeronautics and Space Administration NASA SP-3012 (1964).

At AURORA, photon attenuation experiments indicate that the average photon energy is between 1 and 2 MeV. One wishes to find the dose in $CaF_2$, given a certain silicon equilibrium dose, $D_{Si}$. Also, one ensures that one has CPE by enclosing the TLD in a sufficiently thick aluminum capsule. Assuming CPE,

$$D_{Al} = \frac{(\mu_{en}/\rho)^{Al}_{2 \text{ MeV}}}{(\mu_{en}/\rho)^{Si}_{2 \text{ MeV}}} \; D_{Si} = 0.966 D_{Si} \; . \tag{31}$$

Again assuming that the aluminum-$CaF_2$ system approximates a Bragg-Gray cavity,

$$D_{CaF_2} = \frac{S^{CaF_2}_{600 \text{ keV}}}{S^{Al}_{600 \text{ keV}}} \; D_{Al} = 1.012 D_{Al} \; . \tag{32}$$

Combining equations (31) and (32),

$$D_{CaF_2} = 1.012 \times 0.966 D_{Si} = 0.978 D_{Si} \tag{33}$$

for the dose deposited in $CaF_2$ by AURORA bremsstrahlung.

Now, with the assumption that the TL response of the same TLD is equal for equal absorbed dose regardless of the source, exposure to 0.850 $R(Co^{60})$ will give the same light output as the absorption of 0.978 rads(Si)(AURORA); or

$$0.850 \; X(Co^{60}) = 0.978 D_{Si} (AURORA) \tag{34}$$

whence

$$D_{Si} (AURORA) = 0.870 X(Co^{60}) . \tag{35}$$

This equation (35) is our basic calibration relationship.

By use of the calibration relationship, a whole calibration curve like that in figure 16 can be established. Once it is, however, it need not be repeated, because its shape does not change, even from one TLD production lot to the next. To ensure that the reader is maintained in calibration, it is necessary merely to recheck one point on figure 16 periodically as follows: A representative sampling of AURORA's current lot of TLD's is exposed in a $Co^{60}$ source to an unperturbed exposure of $2.0 \times 10^4$ R. The true exposure at the TLD is

$$0.971 \times 2 \times 10^4 = 1.94 \times 10^4 \text{ R (eq. (26))}.$$

This exposure corresponds to

$$0.870 \times 1.942 \times 10^4 = 1.69 \times 10^4 \text{ rads(Si) (eq. (35))}.$$

Reference to figure 16 reveals that for $P = 1.70 \times 10^4$, $D/P = 0.994$, and $D = 1.69 \times 10^4$ rads(Si). So TLD's exposed to an unperturbed exposure of $2 \times 10^4$ R should yield a reading of exactly $1.70 \times 10^4$ at 1 hr after exposure.

The calibration of the TLD readers is checked periodically, sometimes every day, by reading 10 of these exposed TLD's, correcting for fading, and comparing the mean of the 10 readings to $1.70 \times 10^4$. Since 10 readings are a relatively small sample of the population, the mean P determined this way is typically different from $1.70 \times 10^4$. To test for the statistical significance of this variance, the Student's t-test is used.[12] This is not nearly as laborious as it sounds, since the t-test for the significance of a sample mean is calculated automatically with the HP Model 20 calculator. If the t-test reveals a significant difference between $\bar{P}$ and $1.70 \times 10^4$, the sensitivity of the TLD reader is adjusted to bring it back into calibration.

### 7.2  Silicon-Calorimeter Calibration

Calibration by the silicon calorimeter dispenses with all the assumptions made in the previous paragraphs and compares the TLD reader response directly to an absolute silicon dose standard, irradiated in the AURORA environment. "Absolute" means that the silicon calorimeter need not be calibrated against a known radiation standard. It is necessary merely to be able to measure the change in the resistance of a thermistor very accurately to determine the silicon dose. The construction and operation of this calorimeter is fully described

---

[12]*William Volk, Applied Statistics for Engineers, 2nd Ed., McGraw-Hill Book Co., New York (1958).*

elsewhere.[1]  Briefly, it consists of a tiny thermistor embedded in a silicon pellet that is surrounded by a silicon mantle thick enough to guarantee CPE. The whole calorimeter is thermally isolated from its surroundings.

The rise in temperature of the silicon pellet upon irradiation depends only on the specific heat of silicon and the absorbed dose. The temperature rise is determined by the thermistor, whose (negative) temperature coefficient of resistance is well known. Measurements of $R_0$, the equilibrium resistance of the thermistor, and $\Delta R$, the change in resistance upon irradiation, are the only measurements required to calculate the dose. The resistance parameters are measured with a good Wheatstone bridge (Keithley Model 520). The dose per unit resistance change, $D_{Si}/\Delta R$, is a nonlinear function of $R_0$. To facilitate this calculation, this function was approximated by a fifth-degree polynomial, and the dose calculation is done on the calculator.

For the typical dosimeter calibration, eight TLD's are placed close to the calorimeter (fig. 18), and the whole assembly is exposed to an AURORA pulse. Measurements for $\Delta R$, $R_0$, and $P_1$ to $P_8$ for the dosimeters are put into the calculator. The calculator calculates first the dose as measured by the calorimeter and then the dose corresponding to $P_1$ to $P_8$ using equation (22). It then does a t-test to test whether any variance between $D_{Si}$(calorimeter) and $\bar{D}_{Si}$(TLD) is statistically significant.

When a TLD reader is calibrated by the $Co^{60}$ method, the silicon calorimeter test indicates also that the reader is calibrated. In other words, the two methods do not differ significantly. Both methods are therefore equally valid for calibrating the TLD readers, and both are used routinely.

---

[1]F. H. Attix, *Dosimetry for the Aurora Facility, Final Report*, Naval Research Laboratory, Washington, DC, NRL Memorandum Report 2552, Revised (March 1973).
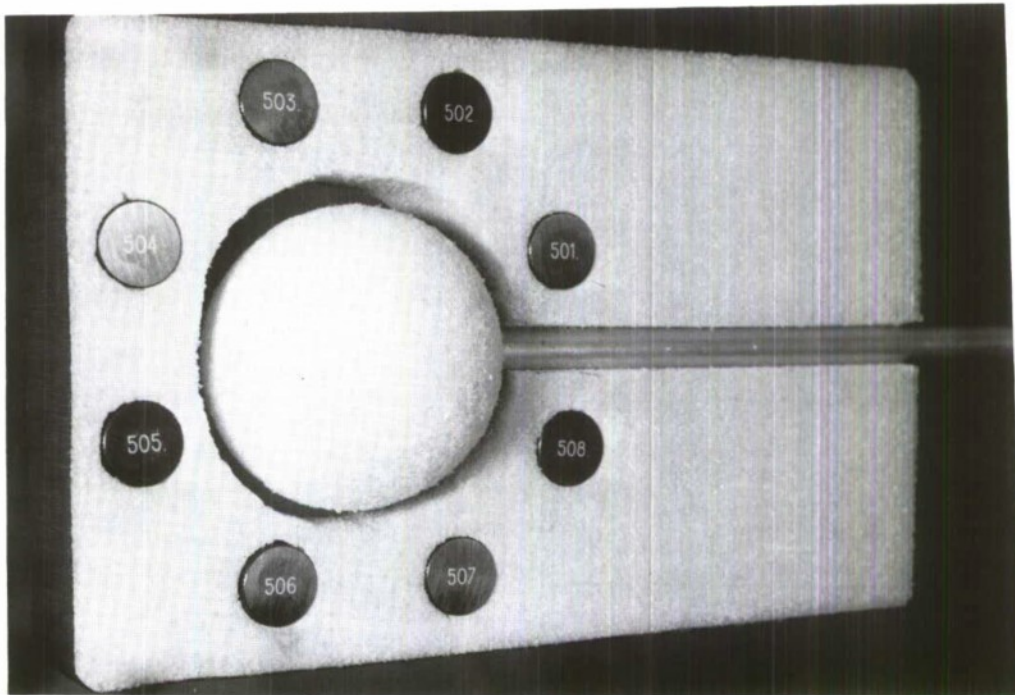
Figure 18.   Absolute silicon calorimeter.

8.   PRECISION AND ACCURACY

   8.1  Definitions

        When a given measurement is  repeated  a  number  of times, the
resulting   values  will,  in  general,  not   agree   exactly.   These
discrepancies  are  caused  by experimental errors.  A measurement  with
small experimental errors has high precision.

        If all measured values are in error by the same  amount, this is
a systematic error.  Measurements with small systematic errors have high
accuracy. [13]

        A   good   measure of the   experimental  error  is  the standard
deviation.  If the experimental errors  are   random,  a  large number of
measurements of the same quantity will  have a normal distribution.   The
standard deviation of a number of normally distributed measurements, $x_i$,
can be estimated by

_____

[13] *Yardley Beers, Introduction  to  the Theory of Error, Addison-Wesley
Publishing Co., Inc., Reading, MA (1956).*

41

$$\left(\frac{\sum\limits_{i} x_i^2 - N\bar{x}^2}{N - 1}\right)^{\frac{1}{2}} \tag{36}$$

where $\bar{x}$ is the arithmetic mean and $N$ is the number of measurements. The probability of a measurement differing from the mean by more than one standard deviation ($1\sigma$) is 0.32; the probability of a $2\sigma$ variance is 0.045.

## 8.2  Precision of TLD Measurements

The percentage standard deviation of a large number of TLD measurements of the same dose has been experimentally determined:[2]

| TLD | $\%s(x)$ |
|-----|----------|
| Teflon disc | 3.15 |
| Solid $CaF_2$:Mn | 5.4 |

This is a measure of the precision of dose measurements made with these TLD's. What this means is that 95 percent of all dose measurements are within $\pm 6.3$ percent of the mean for Teflon disc measurements and within $\pm 11$ percent for solid $CaF_2$:Mn measurements.

## 8.3  Accuracy of TLD Measurements

The amount by which the mean of a large number of measurements differs from the "true" value of the quantity being measured is a measure of the accuracy of the measurement. The accuracy of TLD measurements of dose is difficult to estimate since one does not know, a priori, the systematic errors in the measurements. Two independent measurements of the dose (i.e., use of TLD's calibrated by $Co^{60}$ exposure and use of the silicon calorimeter) generally agree to better than 3 percent. From that fact, one can guess that the accuracy of these measurements is better than 5 percent.

---

[2]S. G. Gorbics, F. H. Attix, and K. Kerris, *Thermoluminescent Dosimeters for High-Dose Applications, Health Physics, 25 (1973), 499.*

## LITERATURE CITED

(1)  F. H. Attix, Dosimetry for the Aurora Facility, Final Report, Naval
     Research Laboratory, Washington, DC, NRL Memorandum Report 2552,
     Revised (March 1973).

(2)  S. G. Gorbics,  F. H. Attix,  and  K. Kerris,  Thermoluminescent
     Dosimeters  for  High-Dose Applications, Health Physics, 25 (1973),
     499.

(3)  F. H. Attix,  W. C. Roesch,  and  E. Tochilin, Radiation Dosimetry,
     2nd Ed., Academic Press, New York (1966).

(4)  F. H. Attix, Basic Gamma-Ray Dosimetry, Health Physics, 15  (1968),
     49.

(5)  Robley D. Evans, The Atomic Nucleus, McGraw-Hill Book Co., New York
     (1955), 723.

(6)  N. Goldstein,  Dose-Rate  Dependence  of  Lithium  Fluoride  for
     Exposures above 15,000 R per Pulse, Health Physics, 22 (1972), 90.

(7)  J. E. Doyle and  W. C. Dickinson,  The  Cerenkov Response of Lucite
     and  Quartz  to  Gamma  and Fast Neutron Radiation,  University  of
     California Lawrence Radiation Laboratory, UCRL-7032 (TID4500) (July
     1962).

(8)  R. K. Durkee, Design and Test of  a  Modular Scintillation Detector
     System,  EG&G,  Santa  Barbara  Division, Technical  Report S-466-R
     (March 1970).

(9)  Ann T. Nelms,  Energy  Loss and Range of Electrons  and  Positrons,
     National Bureau of Standards (U.S.), Circ. 577 (1956).

(10) J. Hubbell,  Photon Cross Sections, Attenuation  Coefficients,  and
     Energy Absorption  Coefficients  from  10 keV  to 100 GeV, National
     Bureau of Standards, NSRDS-NBS29 (August 1969).

(11) M. Berger  and  S. Seltzer,  Tables of Energy Losses and Ranges  of
     Electrons  and  Positrons,  National  Aeronautics  and  Space
     Administration NASA SP-3012 (1964).

(12) William Volk,  Applied  Statistics  for  Engineers,  2nd  Ed.,
     McGraw-Hill Book Co., New York (1958).

(13) Yardley Beers, Introduction to the Theory of  Error, Addison-Wesley
     Publishing Co., Inc., Reading, MA (1956).

DEFENSE DOCUMENTATION CENTER
CAMERON STATION, BUILDING 5
ALEXANDRIA, VA 22314
  ATTN DDC-TCA (12 COPIES)

OFC, CHIEF OF RESEARCH & DEVELOPMENT
USA RSCH & DEV GROUP (EUROPE)
BOX 15
FPR NEW YORK 09510
  ATTN LTC EDWARD E. CHICK
      CHIEF, MATERIALS BRANCH

COMMANDER
US ARMY MATERIEL DEVELOPMENT
 & READINESS COMMAND
5001 EISENHOWER AVENUE
ALEXANDRIA, VA 22333
  ATTN DRCRD, RES, DEV, & ENGR DIRECTORATE

COMMANDER
USA ARMAMENT COMMAND
ROCK ISLAND, IL 61201
  ATTN DRSAR-ASF, FUZE DIV
  ATTN DRSAR-RDF, SYS DEV DIV - FUZES

COMMANDER
USA MISSILE & MUNITIONS CENTER & SCHOOL
REDSTONE ARSENAL, AL 35809
  ATTN ATSK-CTD-F

DIRECTOR
DEFENSE COMMUNICATIONS AGENCY
WASHINGTON, DC 20305
  ATTN CODE 930, MONTE I. BURGETT, JR.

DIRECTOR
DEFENSE NUCLEAR AGENCY
WASHINGTON, DC 20305
  ATTN STTL, TECH LIBRARY
  ATTN RAEV
  ATTN STVL

COMMANDER
FIELD COMMAND
DEFENSE NUCLEAR AGENCY
KIRTLAND AFB, NM 87115
  ATTN FCPR

DIRECTOR
INTERSERVICE NUCLEAR WEAPONS SCHOOL
KIRTLAND AFB, NM 87115
  ATTN DOCUMENT CONTROL

DIRECTOR
JOINT STRAT TGT PLANNING STAFF JCS
OFFUTT AFB
OMAHA, NB 68113
  ATTN JLTW-2

CHIEF
LIVERMORE DIVISION FLD COMMAND DNA
LAWRENCE LIVERMORE LABORATORY
P.O. BOX 808
LIVERMORE, CA 94550
  ATTN FCPRL

WEAPONS SYSTEMS EVALUATION GROUP
400 ARMY NAVY DRIVE
ARLINGTON, VA 22202
  ATTN DOCUMENT CONTROL

COMMANDER
BALLISTIC DEFENSE SYSTEM COMMAND
P.O. BOX 1500
HUNTSVILLE, AL 35807
  ATTN BDMSC-TEN, NOAH J. HURST

COMMANDER
PICATINNY ARSENAL
DOVER, NJ 07801
  ATTN SARPA-ND-N-E

COMMANDER
REDSTONE SCIENTIFIC INFORMATION CTR
US ARMY MISSILE COMMAND
REDSTONE ARSENAL, 35809
  ATTN AMSMI-RBD, CLARA T. ROGERS

SECRETARY OF THE ARMY
WASHINGTON, DC 20310
  ATTN ODUSA OR DANIEL WILLARD

COMMANDER
TRASANA
WHITE SANDS MISSILE RANGE, NM 88002
  ATTN STAA-EAC, FRANCIS N. WINANS

CHIEF
US ARMY COMMUNICATIONS SYS AGENCY
FORT MONMOUTH, NJ 07703
  ATTN SCCM-AD-SV, LIBRARY

COMMANDER
US ARMY ELECTRONICS COMMAND
FORT MONMOUTH, NJ 07703
  ATTN DRSEL-TL-EN, HANS A. BOMKE

COMMANDER-IN-CHIEF
US ARMY EUROPE AND SEVENTH ARMY
APO NEW YORK 09403
  ATTN ODCSE-E, AEAGE-PI

COMMANDER
US ARMY MISSILE COMMAND
REDSTONE ARSENAL
HUNTSVILLE, AL 35809
  ATTN DRCPM-MDTI, CPT JOE A SIMS
  ATTN DRSMI-RGD, VIC RUWE
  ATTN DRCPM-PE-EA, WALLACE O. WAGNER

COMMANDER
US ARMY TEST AND EVALUATION COMD
ABERDEEN PROVING GROUND, MD  21005
  ATTN DRSTE-EL, RICHARD I. KOLCHIN

DIRECTOR
NAVAL RESEARCH LABORATORY
WASHINGTON, DC  20375
  ATTN CODE 5216, HAROLD L. HUGHES

COMMANDER
NAVAL SEA SYSTEMS COMMAND
NAVY DEPARTMENT
WASHINGTON, DC  20362
  ATTN SEA-9931, SAMUEL A. BARHAM

COMMANDER
NAVAL SURFACE WEAPONS CENTER
WHITE OAK, MD  20910
  ATTN CODE WA501, NAVY NUC PRGMS OFF
  ATTN CODE WA50, JOHN H. MALLOY

COMMANDER
NAVAL WEAPONS CENTER
CHINA LAKE, CA  93555
  ATTN CODE 533, TECH LIB

DIRECTOR
STRATEGIC SYSTEMS PROJECT OFFICE
NAVY DEPARTMENT
WASHINGTON, DC  20376
  ATTN NSP-2342, RICHARD L. COLEMAN

AF INSTITUTE OF TECHNOLOGY, AU
WRIGHT-PATTERSON AFB, OH 45433
  ATTN ENP, CHARLES J. BRIDGMAN

AF WEAPONS LABORATORY, AFSC
KIRTLAND AFB, NM  87117
  ATTN ELA
  ATTN SAT

HEADQUARTERS
ELECTRONIC SYSTEMS DIVISION, (AFSC)
L. G. HANSCOM FIELD
BEDFORD, MA  01730
  ATTN YSEV, LTC DAVID C. SPARKS

COMMANDER
FOREIGN TECHNOLOGY DIVISION, AFSC
WRIGHT-PATTERSON AFB, OH  45433
  ATTN ETET, CAPT RICHARD C. HUSEMANN

SAMSO/IN
POST OFFICE BOX 92960
WORLDWAY POSTAL CENTER
LOS ANGELES, CA  90009
  ATTN IND, I. J. JUDY

SAMSO/RS
POST OFFICE BOX 92960
WORLDWAY POSTAL CENTER
LOS ANGELES, CA  90009
  ATTN RSSE, LTC KENNETH L. GILBERT
  ATTN RSE

COMMANDER-IN-CHIEF
STRATEGIC AIR COMMAND
OFFUTT AFB, NB  68113
  ATTN NRI-STINFO LIBRARY

UNIVERSITY OF CALIFORNIA
LAWRENCE LIVERMORE LABORATORY
P.O. BOX 808
LIVERMORE, CA  94550
  ATTN HANS KRUGER, L-96
  ATTN JOSEPH E. KELLER JR.
  ATTN TECH INFO DEPT, L-3

SANDIA LABORATORIES
P.O. BOX 5800
ALBUQUERQUE, NM  87115
  ATTN DOC CON FOR ORG 2110, J. A. HOOD
  ATTN DOC CON FOR 3141, SANDIA RPT COLL

AERONUTRONIC FORD CORPORATION
AEROSPACE & COMMUNICATIONS OPS
AERONUTRONIC DIVISION
FORD & JAMBOREE ROADS
NEWPORT BEACH, CA  92663
  ATTN KEN C. ATTINGER

AEROSPACE CORPORATION
P.O. BOX 92957
LOS ANGELES, CA  90009
  ATTN DONALD A. MCPHERSON

BELL AEROSPACE COMPANY
DIVISION OF TEXTRON, INC.
P.O. BOX 1
BUFFALO, NY  14240
  ATTN MARTIN A. HENRY

BENDIX CORPORATION, THE
COMMUNICATION DIVISION
EAST JOPPA ROAD - TOWSON
BALTIMORE, MD  21204
  ATTN DOCUMENT CONTROL

BOEING COMPANY, THE
P.O. BOX 3707
SEATTLE, WA  98124
  ATTN ROBERT S. CALDWELL, 2R-00
  ATTN AEROSPACE LIBRARY

BOOZ-ALLEN AND HAMILTON, INC.
106 APPLE STREET
NEW SHREWSBURY, NJ  07724
  ATTN RAYMOND J. CHRISNER

CHARLES STARK DRAPER LABORATORY, INC.
68 ALBANY STREET
CAMBRIDGE, MA  02139
 ATTN KENNETH FERTIG

CUTLER-HAMMER, INC.
AIL DIVISION
COMAC ROAD
DEER PARK, NY  11729
 ATTN CENTRAL TECH FILES, ANNE ANTHONY

EFFECTS TECHNOLOGY, INC.
5383 HOLISTER AVENUE
SANTA BARBARA, CA  93105
 ATTN EDWARD JOHN STEELE

FAIRCHILD INDUSTRIES, INC.
SHERMAN FAIRCHILD TECHNOLOGY CENTER
20301 CENTURY BOULEVARD
GERMANTOWN, MD  20767
 ATTN MGR CONFIG DATA & STANDARDS

GENERAL DYNAMICS CORPORATION
ELECTRONICS DIV ORLANDO OPERATIONS
P.O. BOX 2566
ORLANDO, FL  32802
 ATTN D. W. COLEMAN

GENERAL ELECTRIC COMPANY
SPACE DIVISION
VALLEY FORGE SPACE CENTER
GODDARD BLVD KING OF PRUSSIA
P.O. BOX 8555
PHILADELPHIA, PA  19101
 ATTN LARRY I. CHASEN

GENERAL ELECTRIC COMPANY
ORDNANCE SYSTEMS
100 PLASTICS AVENUE
PITTSFIELD, MA  01201
 ATTN JOSEPH J. REIDL

GENERAL ELECTRIC COMPANY
WASHINGTON OFFICE
AEROSPACE GRP STRAT PLANNING & PRGMS OPS
777 14TH STREET, NW
WASHINGTON, DC  20005
 ATTN DASIAC, WILLIAM ALFONTE

GENERAL ELECTRIC COMPANY
TEMPO-CENTER FOR ADVANCED STUDIES
816 STATE STREET (P.O. DRAWER QQ)
SANTA BARBARA, CA  93102
 ATTN DASIAC

GENERAL ELECTRIC COMPANY
P.O. BOX 1122
SYRACUSE, NY  13201
 ATTN CSP 6-7, RICHARD C. FRIES

GENERAL ELECTRIC COMPANY-TEMPO
ATTN: DASIAC
C/O DEFENSE NUCLEAR AGENCY
6801 TELEGRAPH ROAD
ALEXANDRIA, VA  22310
 ATTN WILLIAM ALFONTE

GRUMMAN AEROSAPCE CORPORATION
SOUTH OYSTER BAY ROAD
BETHPAGE, NY  11714
 ATTN JERRY ROGERS, DEPT 533

GTE SYLVANIA, INC.
189 B. STREET
NEEDHAM HEIGHTS, MA  02194
 ATTN H & V GROUP, MARIO A. NUREFURA

HARRIS CORPORATION
HARRIS SEMICONDUCTOR DIVISION
P.O. BOX 883
MELBOURNE, FL  32901
 ATTN WAYNE E. ABARE, MS 16-111
 ATTN T. L. CLARK, MS 4040

HONEYWELL INCORPORATED
GOVERNMENT AND AERONAUTICAL
PRODUCTS DIVISION
2600 RIDGEWAY PARKWAY
MINNEAPOLIS, MN  55413
 ATTN RONALD R. JOHNSON, A1622

HONEYWELL INCORPORATED
RADIATION CENTER
2 FORBES ROAD
LEXINGTON, MA  02173
 ATTN TECHNICAL LIBRARY

HUGHES AIRCRAFT COMPANY
CENTINELA AND TEALE
CULVER CITY, CA  90230
 ATTN KENNETH R. WALKER, MS D157

INTELCOM RAD TECH
P.O. BOX 80187
SAN DIEGO, CA  92138
 ATTN RALPH H. STAHL
 ATTN MDC
 ATTN R. L. MERTZ

KAMAN SCIENCES CORPORATION
P.O. BOX 7463
COLORADO SPRINGS, CO  80933
 ATTN DONALD H. BRYCE

LITTON SYSTEMS, INC.
GUIDANCE & CONTROL SYSTEMS DIVISION
5500 CANOGA AVENUE
WOODLAND HILLS, CA  91364
 ATTN JOHN P. RETZLER

LOCKHEED MISSILES & SPACE CO INC
P.O. BOX 504
SUNNYVALE, CA  94088
 ATTN D. M. TELLEP, DEPT 81-01

LOCKHEED MISSILES AND SPACE COMPANY
3251 HANOVER STREET
PALO ALTO, CA  94304
 ATTN TECH INFO CIR D/COLL

LTV AEROSPACE CORPORATION
VOUGHT SYSTEMS DIVISION
P.O. BOX 6267
DALLAS, TX 75222
 ATTN TECHNICAL DATA CENTER

M.I.T. LINCOLN LABORATORY
P.O. BOX 73
LEXINGTON, MA  02173
 ATTN LEONA LOUGHLIN, LIBRARIAN A-082

MARTIN MARIETTA AEROSPACE
ORLANDO DIVISION
P.O. BOX 5837
ORLANDO, FL  32805
 ATTN WILLIAM W. MRAS, MP-413

RAYTHEON COMPANY
HARTWELL ROAD
BEDFORD, MA  01730
 ATTN GAJANAN H. JOSHI, RADAR SYS LAB

RCA CORPORATION
GOVERNMENT & COMMERCIAL SYSTEMS
ASTRO ELECTRONICS DIVISION
P.O. BOX 800, LOCUST CORNER
PRINCETON, NJ  08540
 ATTN GEORGE J. BRUCKER

ROCKWELL INTERNATIONAL CORPORATION
3370 MIRALOMA AVENUE
ANAHEIM, CA  92803
 ATTN K. F. HULL

SANDERS ASSOCIATES, INC.
95 CANAL STREET
NASHUA, NH  03060
 ATTN MDE L. AITEL, NCA 1-3236

SCIENCE APPLICATIONS, INC.
P.O. BOX 2351
LA JOLLA, CA  92038
 ATTN J. ROBERT BEYSTER
 ATTN LARRY SCOTT

STANFORD RESEARCH INSTITUTE
333 RAVENSWOOD AVENUE
MENLO PARK, CA  94025
 ATTN ROBERT A. ARMISTEAD

THE SINGER COMPANY (DATA SYSTEMS)
150 TOTOWA ROAD
WAYNE, NJ  07470
 ATTN TECH INFO CENTER

TRW SYSTEMS GROUP
ONE SPACE PARK
REDONDO BEACH, CA  90278
 ATTN TECH INFO CENTER/S-1930
 ATTN A. M. LIEBSCHUTZ, R1-1162
 ATTN A. A. WITTELES, MS R1-1120
 ATTN AARON H. NAREVSKY, R1-2144

TRW SYSTEMS GROUP
SAN BERNARDINO OPERATIONS
P.O. BOX 1310
SAN BERNARDINO, CA  92402
 ATTN H. S. JENSEN

VAN LINT, VICTOR A. J. (CONSULTANT)
MISSION RESEARCH CORPORATION
SAN DIEGO, CA  92111
 ATTN V. A. J. VAN LINT

HARRY DIAMOND LABORATORIES
 ATTN MCGREGOR, THOMAS, COL, COMMANDING
      OFFICER/FLYER, I.N./LANDIS, P.E./
      SOMMER, H./CONRAD, E.E.
 ATTN CARTER, W.W., DR., ACTING TECHNICAL
      DIRECTOR/MARCUS, S.M.
 ATTN KIMMEL, S., IO
 ATTN CHIEF, 0021
 ATTN CHIEF, 0022
 ATTN CHIEF, LAB 100
 ATTN CHIEF, LAB 200
 ATTN CHIEF, LAB 300
 ATTN CHIEF, LAB 400
 ATTN CHIEF, LAB 500
 ATTN CHIEF, LAB 600
 ATTN CHIEF, DIV 700
 ATTN CHIEF, DIV 800
 ATTN CHIEF, LAB 900
 ATTN CHIEF, LAB 1000
 ATTN RECORD COPY, BR 041
 ATTN HDL LIBRARY (3 COPIES)
 ATTN CHAIRMAN, EDITORIAL COMMITTEE
 ATTN CHIEF, 047
 ATTN TECH REPORTS, 013
 ATTN PATENT LAW BRANCH, 071
 ATTN MCLAUGHLIN, P.W., 741
 ATTN WIMENITZ, F. N., 0024
 ATTN MCCOSKEY, R. E., 200
 ATTN KERRIS, K. G. (50 COPIES)